1-1-2001

The disorder-to-order phase transition in poly(styrene-block-N-butyl methacrylate) : the effect of pressure.

Michael Anthony Pollard
University of Massachusetts Amherst

THE DISORDER-TO-ORDER PHASE TRANSITION IN POLY(STYRENE-*BLOCK*-N-BUTYL METHACRYLATE): THE EFFECT OF PRESSURE

A Dissertation Presented

by

MICHAEL ANTHONY POLLARD

Submitted to the Graduate School of the
University of Massachusetts Amherst in partial fulfillment
of the requirements for the degree of

DOCTOR OF PHILOSOPHY

September 2001

Polymer Science and Engineering

THE DISORDER-TO-ORDER PHASE TRANSITION IN POLY(STYRENE-*BLOCK*-N-BUTYL METHACRYLATE): THE EFFECT OF PRESSURE

A Dissertation Presented

by

MICHAEL ANTHONY POLLARD

Approved as to style and content by:

T. Russell, Chair

M. Muthukumar, Member

J. Watkins, Member

T. McCarthy, Department Head

Polymer Science and Engineering

ACKNOWLEDGEMENTS

A number of people were instrumental building up the foundation for the work presented in thesis. They provided technical expertise, a stimulating research atmosphere, and a collegiate working environment. I am indebted to the following people, in particular, for their role in shaping my professional and personal growth over the course of five years: Prof. T. Russell, Prof. M. Muthukumar, Prof. J. Watkins, and Prof. D. Hoagland; Dr. P. Mansky, Dr. O. K. C. Tsui, Dr. T. Thurn-Albrecht, and Dr. T. Kerle; A.-V. Ruzette, and Prof. A. Mayes; Dr. A. Waddon, and L. Raboin; J. DeRouchey, G. Brown, D. Flanagan, and G. Menges.

ABSTRACT

THE DISORDER-TO-ORDER PHASE TRANSITION

IN POLY(STYRENE-*BLOCK*-N-BUTYL METHACRYLATE):

THE EFFECT OF PRESSURE

SEPTEMBER 2001

MICHAEL A. POLLARD, B. S., UNIVERSITY OF SOUTHERN MISSISSIPPI

M. S., UNIVERSITY OF MASSACHUSETTS AMHERST

Ph. D., UNIVERSITY OF MASSACHUSETTS AMHERST

Directed by: Thomas P. Russell

The effect of hydrostatic pressure on the lower disorder-to-order transition (LDOT) in poly(*d*-styrene-*block*-n-butyl methacrylate) having symmetric and asymmetric block lengths was investigated by *in situ* small-angle neutron scattering (SANS). Currently, linear diblock copolymers having styrenic and methacrylic monomers are the only systems that display a thermally accessible phase transition from the disordered homogeneous melt to the ordered microphase-separated state upon *heating*. The location of this phase transition was mapped as a function of temperature and pressure by analyzing one-dimensional SANS intensities, where discontinuities in the width and height of the scattering peak indicated the traversal of the transition isothermally or isobarically.

The T-P phase diagram of p(*d*-S-*b*-nBMA) built using this method shows an expansion of the disordered, homogenous region with increasing pressure. For the

diblock copolymer with a lamellar morphology and $M_w = 8.5 \times 10^4$, the slope of the phase transition line was ~ 150 K/kbar, and was approximately linear over a range of 1 kbar. Increasing the molecular weight of p(*d*-S-*b*-nBMA) resulted in a vertical shift of the phase transition line in the phase diagram and no detectable change in slope. Similar effects were observed for diblock copolymers with a cylindrical morphology. The bulk enthalpy and volume changes at the phase transition, which dictate the pressure coefficient for a one component system, were either at the limit of experimental resolution or unobservable due to kinetic factors. In-situ X-ray reflectivity experiments, however, showed a significantly reduced thermal expansion coefficient in the disordered phase and a discontinuous increase in film thickness as a function of temperature at the bulk LDOT.

The pressure coefficient, dT_{LDOT}/dP, for these materials is greater by a factor of five than currently observed in diblock copolymers with conventional UODT phase behavior, i.e. ordering upon *cooling*. This dramatic phase behavior allows rapid and convenient access to the order-disorder phase transition, isothermally, and suggests that LDOT block copolymers could be employed in blend and multi-component systems as minor components to impart pressure-induced compatibilization, surface activity, or flow properties.

TABLE OF CONTENTS

ACKNOWLEDGEMENTS iv

ABSTRACT v

LIST OF FIGURES viii

CHAPTER

1. INTRODUCTION 1

    A. Background 1
    B. Methods and Materials 4
    C. References 6

2. PRESSURE DEPENDENCE OF LDOT 8

    A. Initial SANS Experiments 8
    B. Further SANS Experiments 13
    C. Phase Diagram 15
    D. Summary 16
    E. References 17
    F. Figures 18

3. VOLUME AND HEAT EFFECTS 28

    A. X-Ray Reflectivity 28
    B. Differential Scanning Calorimetry 31
    C. Polarized Light Microscopy 35
    D. Discussion 36
    E. References 37
    F. Figures 39

4. PHASE DIAGRAM OF p(*d*-S-*b*-nBMA) 43

    A. Schematic Phase Diagrams 43
    B. Experimental Studies 46
    C. Discussion 48
    D. References 58
    E. Figures 61

5. CONCLUSIONS 67

BIBLIOGRAPHY 71

LIST OF FIGURES

Figure		Page
2.1	SANS profiles, 85k	18
2.2	Peak parameters, 85k	19
2.3	SANS profiles, 85k	20
2.4	Peak parameters, 85k	21
2.5	Peak parameters, summary	22
2.6	SANS profiles, 134k	23
2.7	Temperature-pressure superposition, 85k	24
2.8	Pressure coefficient, 85k	25
2.9	Phase diagram, 96k	26
2.10	Phase diagram, summary	27
3.1	Reflectivity profiles, 85k	39
3.2	Film thickness discontinuity, 85k	40
3.3	DSC, 75k	41
3.4	Ordering kinetics, 75k & 78k	42
4.1	Schematic block copolymer phase diagrams	61
4.2	Transition temperatures, UODT and LDOT	62
4.3	Best fit of transition temperatures	63
4.4	Flory-Huggins parameters in LCST blends	64
4.5	Deuteration effect in p(S-*b*-nBMA)	65

CHAPTER 1

INTRODUCTION

A. Background

Block copolymers are created by joining two homopolymer chains, $(\text{-A-})_x$ and $(\text{-B-})_y$ together covalently to form $(\text{-A-B-})_N$. The presence of the junction point restricts phase separation when there are strong repulsions between A and B blocks. As a result, the size of the phase-separated domains is determined only by the chain length, typically tens of nanometers. A variety of periodic structures will then spontaneously form as a result of the packing between A and B domains. Classically, these equilibrium morphologies consist of either spheres, cylinders, or lamellae, depending on the fraction, f_A, of A monomers relative to B monomers. Due to the complexity of this 'self-assembling' process, and the variety of solution- and melt-based structures that develop naturally out of this simple linear chain architecture, block copolymers have been of keen interest in the scientific and industrial communities for many decades. An extensive literature covering phase behavior and properties is summarized in several excellent reviews.[1-4]

A theme which is of continuing interest in the study of linear diblock copolymers is their phase behavior. Guided by theory, the phase behavior is usually characterized in terms of the product (χN), where χ_{AB} is the Flory-Huggins interaction parameter, and N is the chain length. This parametrization reflects the thermodynamic forces that are competing for dominance of the free energy. Microphase separation is driven by the chemical incompatibility between A and B monomers, but the chain-stretching and

loss of translational freedom that accompanies microphase separation is entropically unfavored. By selecting highly incompatible monomers, the strong repulsions between A and B will dominate the free energy for all but the shortest chains. This is the strong-segregation regime which is described by the condition $(\chi N) >> 10$. Here, the microphase-separated (ordered) state is most stable. Alternatively, by selecting compatible monomers, so that the condition $(\chi N) << 10$ is met, the entropy will dominate since the interaction energy is too weak to force microphase separation. In this situation, the phase-mixed (disordered) state is the most stable.

A fine balance exists between the energetic and entropic forces when $(\chi N) \sim 10$. In this regime, the phase transition separating the ordered and disordered states can be accessed thermally. This allows the state of the block copolymer to be controlled simply by adjusting the temperature. Since the interaction energy assumes form, $\chi \sim 1/T$, a block copolymer with properly chosen molecular weight and interaction energies will undergo this transition from the homogeneous state to the microphase separated state when cooled. This phase transition is denoted the microphase separation transition (MST) or the order-disorder transition (ODT). When a diblock copolymer is cooled into the ordered state, the A blocks will locally segregate from the B blocks and subsequently form an extendend lattice as these domains pack together. These anisotropic structures will develop during an experimentally relevant time scale, and give rise to rapid and discontinuous changes in the mechanical and optical properties. Dynamical mechanical spectroscopy and depolarized light scattering are currently widely employed to study these property changes at the order-disorder transition.[5-6] Since a block copolymer in the ordered phase can be melted by raising its temperature, we denote this phase transition the upper order-disorder transition

(UODT) by analagy with the UCST phase behavior observed in two-component mixtures.

In a striking deviation from this classical behavior, block copolymers composed of poly(styrene) and poly(n-butyl methacrylate) were shown to possess an inverted temperature dependence of this transition.[7] In this diblock copolymer system, denoted p(S-*b*-nBMA), the disordered state is more stable than the ordered state at ambient temperatures, but becomes progessively destabilized as temperature is increased. In this case the diblock copolymer will undergo the transition from the homogeneous state to the microphase separated state when *heated*. Consequently, the mechanical and optical property changes are reversed as well, with the unusual result that a viscous, flowable melt will rapidly become more rigid when heated above its ordering transition.[8] By analogy with the LCST phase behavior observed in polymer mixures, we label this the lower disorder-order transition (LDOT). Currently, diblock copolymers composed of styrenic and methacrylate blocks are the only systems with identifiable and thermally accessible transition of this type.

Many questions emerged from these observation of LCST-type phase behavior in a diblock copolymer. Since diblock copolymer phase behavior often mirrors that observed in the parent homopolymers, one relevant question is, to what extent are the mechanisms responsible for the LCST in blend systems also present in poly(styrene-*block*-n-butyl metharylate). Further, to what extent can this understanding be used to control and manipulate this kind of phase behavior? In studies of miscible blends with an LCST, a common goal is to identify the molecular origin of the ambient temperature compatibility and to understand why there is a tendency to phase separate at higher temperatures. Several pertinent factors have emerged from these

studies which are commonly invoked in the literature to explain high-temperature demixing. These include hydrogen-bonding, or directional-specific interactions, and the "equation-of-state" effects due to the finite compressibility of the mixture.[9-10]

Since there are only weak interactions in styrene and n-butyl methacrylate monomers, we intuitively expect that equation of state effects, or nonideal excess mixing volumes, plays a major role in the case of poly(styrene-*block*-n-butyl methacrylate). The experimental studies described in this dissertation were directly motivated by the idea that equation-of-state effects dominate the phase behavior in this system. This is a recurring theme in the literature, where presently there is a keen interest to describe and illustrate how these mixing nonidealities can have dramatic effects on the phase behavior of simple polymer blends.[11-13] A first step was undertaken to explore this idea in the p(S-*b*-nBMA) diblock copolymers by examining the response to pressure exhibited by the low temperature disordered phase and the high temperature ordered phase. A particular interest was to use the phase information from these studies to build a T–P phase diagram, and contrast its behavior with the form typical of the conventional UODT. With this background, initial experiments were begun as described Chapter 2.

B. Methods and Materials

Only a limited set of analytical tools are available to study high pressure effects in polymeric materials. Phase behavior studies of block copolymers have in the past used high-pressure dilatometry, small-angle X-ray scattering (SAXS), and small-angle neutron scattering (SANS). The former technique is typically hampered by requiring

unrecoverable and large quantities of material (> 1 gm), and equipment design that tends to exacerbate user error and therefore require significant expertise. The two scattering techniques require high contrast for detection. In SAXS, the presence of the phase separated domains gives rise to a Bragg reflection that is characteristic of the domain spacing,[14] but a sufficient difference in density between domains is required to generate scattering contrast. The parent homopolymers of p(S-*b*-nBMA) unfortunately have similar densities and are not expected to have a high scattering contrast. This can be effectively circumvented only through the increased flux available at a synchrotron source. SANS also requires sufficient contrast in the atomic scattering lengths, which can usually be provided by replacing hydrogen atoms in the domain of interest with deuterium atoms. Although this perturbs the thermodynamics to some extent, and must be accounted for, additional flexibility is offered by the convenience of user-supported neutron scattering sources which feature high-pressure cells and equipment suitable for in-situ measurements. The use of SANS coupled with deuterium-labelling in the diblock copolymers was therefore deemed the most suitable approach for investigating pressure effects on the phase behavior. Further measurements, as described in Chapter III, were conducted using equipment available in the Polymer Science and Engineering Department, including optical microscopy, calorimetry, and X-ray reflectivity.

The diblock copolymers used throughout the experiments were synthesized and provided by Prof. Gallot of the Institut Sadron. In order to provide contrast for neutron scattering measurements, perdeuterated styrene was used in the synthesis. All diblock copolymers were synthesized using stepwise anionic polymerization, using perdeutered styrene and n-butyl methacrylate monomers. The characteristics of these

block polymers are listed below. LAM and CYL refer to the lamellar, cylindrical morphologies. LDOTs were determined either by SANS or optical microscopy.

$M/10^4$	PS wt%	Morphology	LDOT
6.8	51	LAM	225
7.5	47	LAM	180
7.8	49	LAM	165
8.5	~50	LAM	155
9.6	~50	LAM	100
17.0	55	LAM	-
9.5	29	CYL	>250
13.4	29	CYL	125
14.6	71	CYL	< Tg

C. References

[1]Morphologies of block copolymers. Schulz, M.; Bates, F. in *Physical Properties of Polymers*, Mark J., Ed., Ch 32, **1999**, 427.

[2]Phase morphology in block copolymer systems. Thomas, E.; Lescanec, L. *Phil. Trans. R. Soc. Lond. A*, **1994**, *348*, 149.

[3]Polymer-polymer phase behavior. Bates, F. S. *Science* **1991**, *251*, 898.

[4]Review. Bates, F. S.; Fredrickson, G. H. *Annu. Rev. Phys. Chem.* **1990**, *41*, 525.

[5]Order and disorder in symmetric diblock copolymer melts. Rosedale, J.; Bates, F.; Almdal, K.; Mortensen, K.; Wignall, G. *Macro.*, **1995**, *28*, 1429.

[6]Birefringence detection of the order-to-disorder trnasition in block copolymer liquids. Balsara, N; Perahia, D.; Safinya, C.; Tirrell, M.; Lodge, T. *Macro.*, **1992**, *25*, 3896.

[7]Russell, T. P.; Karis, T. E.; Gallot, Y.; Mayes, A. M. *Nature* 1994, *368*, 729.

[8]Rheology of the lower critical ordering transition. Karis, T. E.; Russell, T. P.; Gallot, Y.; Mayes, A. M. *Macro.* 1995, *28*, 1129.

[9]Free volume and polymer solubility. A qualitative view. Patterson, D. *Macro.*, 1969, 2, 672.

[10]Aspects of polymer-polymer thermodynamics. McMaster, L. *Macro.*, 1973, *6*, 760.

[11]Chain-Packing effects in the thermodynamics of polymers. Londono, J.; Maranas, J.; Mondello, M.; Habenschuss, A.; Grest, G.; Debenedetti, P.; Graessley, W.; Kumar, S. *J. Polym. Sci., Polym. Phys.* **1998**, *36*, 3001.

[12]Regular and irregular mixing in blends of saturated hydrocarbons in polymers. Graessley, W.; Krishnamoorti, R.; Reichart, G.; Balsara, N.; Fetters, L.; Lohse, D. *Macro.*, **1995**, 1260.

[13]Effect of molecular structure on the thermodynamics of block copolymer melts. Lin, C, Jonnalagadda, S.; Kesani, P.; Dai, H.; Balsara, N. *Macro.*, **1994**, *27*, 7769.

[14]Block copolymers near the microphase separation transition. 3. Small-angle neutron scattering study of the homogeneous melt state. Bates, F.; Hartney, M. *Macro.*, 1985, *18*, 2478.

CHAPTER 2

PRESSURE DEPENDENCE OF THE LDOT

A. Initial SANS Experiments

Objectives. A primary objective of this thesis is to explore the phase diagram of PS-PBMA block copolymers, in particular to study the effect of pressure on the LDOT observed in these materials. The transition temperature is a function of molecular weight, as shown in Figure 4.2, and is accessible thermally for a range of molecular weights between approximately 6.5 and 10.0 x 10^4 g/mol. Since there are dramatic bulk property changes occurring across the transition, it will be of interest to determine the slope, dT_{LDOT}/dP, and curvature of the phase transition line throughout the experimentally accessible pressure range. We focus initially on diblocks with symmetric block lengths, where the styrene volume fraction, ϕ_{dPS}, is approximately 1/2. The effect of molecular weight, N, on the pressure coefficient will also be examined. Small-angle neutron scattering (SANS) was chosen as the principle experimental technique in these studies. SANS probes the relevant length scale in block copolymer microstructures, and allows a nondestructive in-situ evaluation of the phase state as a function of both pressure and temperature.

Experimental. Symmetric block copolymers of perdeuterated polystyrene and poly(n-butyl methacrylate) were synthesized using high-vacuum anionic polymerization techniques. Four diblock copolymers, with M_w = 6.8 x 10^4, 7.8 x 10^4, and 8.5 x 10^4, were chosen for SANS measurements. These copolymers have polydispersities less than 1.08 and dPS volume fractions between 0.47 and 0.51

(lamellar morphology). Additionally, a copolymer with $M_w = 1.3 \times 10^5$ and $\phi_{dPS} = 0.29$ (cylindrical morphology) was selected to examine block asymmetry. For convenience, these are labelled throughout as 68k, 78k, 85k, and 134k. Samples were melt-pressed into discs with a thickness of 1.2 mm and a diameter of 16 mm, corresponding to the dimensional requirements of the sample cell. The small-angle neutron scattering (SANS) measurements were performed at the Cold Neutron Research Facility at the National Institute of Standards and Technology on beamline NG-3. This beamline is equipped with a hydraulic pressure cell designed for in-situ high pressure SANS. It has an operating range from ambient conditions to 250 °C and 1000 bar. In this cell design the sample is held to constant thickness by metal spacers and two transparent sapphire windows and is surrounded in the radial direction by a teflon gasket through which pressure is transmitted by the surrounding silicone oil. This provides an isotropic compression in the scattering direction. The instrument configuration for all experiments was $\lambda = 6$ Å and $\Delta\lambda/\lambda = 0.15$, at a sample-detector distance of 9 m.

Measurements were taken from 130 to 190 °C and from 10 to 1000 bar, by first increasing pressure isothermally in increments of 0.17 kbar, then incrementing temperature by 10 °C and repeating the pressure sweep. A subsequent calibration of the temperature control and feedback system showed that the effective sample temperature during these experiments was 150 to 225 °C, with 12 °C increments between sweeps. Equilibrium waiting times between data collection at each temperature and pressure was at least ten minutes. Reproducibility was verified by repeating several measurements at the conclusion of each temperature sweep, and size exclusion chromatography showed no changes in the molecular weight distribution as a result of the high temperatures and pressures. The two-dimensional scattering

patterns were azimuthally averaged to one-dimension, and then corrected for background and detector inhomogeneity. In some cases, intensity was scaled to an absolute level using several available intensity standards. The results are shown as profiles of relative or absolute Intensity, I (cm^{-1}) versus Wavevector, Q ($Å^{-1}$), where $Q = (4\pi/\lambda) \sin(\phi/2)$. The peak in the scattering profiles was characterized by fitting to a lorentzian function, where the peak width, σ^*, peak height, I^*, and maximum wavevector, Q^*, were adjustable parameters.

Results. A typical series of SANS results as a function of temperature at fixed pressure of 170 bar is shown in Figure 2.1 for the 85k p(*d*-S-*b*-nBMA). At low temperatures the profile shows a diffuse scattering maximum at Q = 0.022 $Å^{-1}$, a characteristic length scale associated with the block copolymer in the disordered state. As the temperature is increased, the peak sharpens and intensifies; this trend indicates that increasing the temperature results in decreasing compatibility, and signals that an LDOT will appear at higher temperatures. At 188 °C, a discontinuous change is observed in the peak intensity and width, indicating that the LDOT phase boundary has been traversed, and that the copolymer is microphase separated.

The breadth of the scattering maximum is often employed as a convenient means to characterize the phase state of block copolymers. At the ordering transition, the full width at half-maximum (FWHM) is expected to undergo an abrupt decrease. Additionally, the peak intensity at the scattering maximum, I^*, is expected to show a discontinuous increase. Both features are observed in the scattering profiles in Figure 2.1 and indicate an LDOT for this material at approximately 180 °C. Figure 2.2 shows the FWHM, and peak intensity, I^*, as a function of temperature at 170 bar for the 85k

p(*d*-S-*b*-nBMA). The discontinuity at 180 °C is clearly identified as the LDOT at this pressure.

The effect of pressure on the phase transition temperature is shown in Figure 2.3, where the profiles are shown for increasing pressures at a fixed temperature of 190 °C. At the chosen temperature, the 85k p(*d*-S-*b*-nBMA) is in the ordered state at lower pressures, as characterized by the sharp reflection at Q = 0.021 $Å^{-1}$, and a second order reflection at approximately Q = 0.042 $Å^{-1}$. As the pressure is increased, the intensity of the peak decreases. At 340 bar, a sudden decrease of the peak width and loss of the higher order peak indicates that the phase transition has been traversed isothermally and the copolymer is in the disordered state. Further application of pressure continues to broaden the peak and lower the peak intensity. These trends are summarized in Figure 2.4, where the peak width and height is shown as a function of pressure at 190 °C. The discontinuity at 340 bar can be identified as the disordering pressure, or LODP, at this temperature. This is consistent with the LDOT shown in the Figure 2.3 within the experimental resolution.

The full array of T–P data is summarized in Figure 2.5, where the FWHM, I*, and Q* are shown as a function of temperature and pressure. To facilitate the comparison of data sets, the data are shown in an isobaric representation, although the data were collected by sweeping the pressure isothermally. A dotted line indicates the approximate LDOT as observed from the discontinuities in the FWHM and I*. The interesection of this dotted line with the two lowest data sets indicates the very strong effect of pressure in shifting the LDOT to much higher temperatures. As seen in the lowest pressure data set, the ambient pressure (14 bar) ordering temperature is approximately 158 °C, while at 170 bar the transition shifts to approximately 182 °C.

At higher pressures, the transition becomes inaccessible, shifting to temperatures beyond the reach of the experiment. Despite the coarse temperature and pressure increments used in this experiment, these results indicate that the LDOT increases very strongly with the application of moderate pressures.

Similar results were obtained for the other molecular weights. For the 78k copolymer, the ambient pressure LDOT was approximately 15 °C higher than for the 85k copolymer, and similarly strong pressure sensitivity was observed. For the 68k copolymer, the disordered state prevailed throughout the temperature and pressure range, with the ambient pressure LDOT beyond experimental range (>225 °C). In the case of the asymmetric 134k copolymer, the material was ordered throughout the entire temperature range at ambient pressures. Glass formation prevented thermal access to the LDOT at the expected temperature of ~110 °C. Rapid isothermal disordering was observed, however, by application of pressure at temperatures above T_g, as shown in Figure 2.6. The peak broadening and loss of higher order peaks at 850 bar indicates that the cylindrical morphology has been disordered isothermally. In this case the pressure dependence of the LDOT in a cylindrical morphology is similar to that observed in the lamellar morphology. Importantly, this result shows that the application of pressure opened a window to the disordered state, which was thermally inaccessible at ambient pressures.

Determination of Pressure Coefficient, dT_{LDOT}/dP. Examination of the temperature dependence of the peak parameters in Figure 2.5 indicates that the curves appear to be slices of a master curve, shifted along the horizontal axis. This may reflect the fact that the shape of the scattering peak undergoes a similar shape change at the phase transition, regardless of the absolute value of the pressure at which it occurs. By

shifting the constant pressure curves along the temperature axis through an amount $T_{shift} = T - \alpha P$, where P is the pressure of that data range and α is a shift coefficient, it appears to generate a universal curve, as shown in Figure 2.7. Significant overlap is observed for this temperature-pressure superposition in the three scattering profile parameters I*, FWHM, and Q*. Notably, the magnitude of the shift, α, quantifies the equivalence in temperature and pressure, and provides an estimate of the pressure coefficient, dT_{LDOT}/dP. Figure 2.8 shows the shift along the temperature axis as a function of pressure for the 85k material. A best fit of this line yields $\alpha = 147 \pm 7$ °C for the 85k material. The magnitude of the pressure coefficient is estimated to be of order 150 °C/kbar.

B. Further SANS Experiments

Objective. The results of the SANS experiments shown above indicate a very strong, positive pressure coefficient for p(*d*-S-*b*-nBMA) block copolymers. However, we would like to test the validity of the superpositioning procedure used to estimate the coefficient by conducting additional SANS measurements with a finer temperature and pressure resolution. This will allow a quantitative determination of the LDOT slope in the phase diagram of p(*d*-S-*b*-nBMA).

Experimental. In order to examine the isothermal transition at a moderate temperature, the 96k material was chosen for these experiments. Based on the molecular weight dependence, the LDOT for this material was expected to be at ~ 100 °C. With the expected pressure coefficient of ~145 °C/kbar, this allowed moderate pressures to be used for observing the isothermal disordering at temperatures lower

than 170 °C. Sample preparation and experimental conditions were the same as those reported above. The ordered material was first equilibrated in situ at 140 °C and ambient pressure. Next, pressure was increased in increments of 20 bar through the isothermal transition and into the disordered state. After disordering, pressure was decreased in 20 bar increments to return to the ordered state and examine the reversibility of the transition. This pressurization procedure was repeated at 160 °C.

Results. Results obtained for the 96k material are summarized in Figure 2.9, where a T–P diagram shows the equilibrium state as a function of temperature and pressure. The ordered (ORD) and disordered (DIS) states were identified by locating the discontinuities in the fitted peak parameters FWHM and I*. The pressure coefficient calculated from the two LDOTs in figure 2.9 gives $\Delta T/\Delta P$ = (20 °C)/(0.130 kbar) = 154 °C/kbar. An error of ± 20 °C/kbar is estimated from the observed temperature variation of ± 1.5 °C during the experiment. This result is in good agreement with the estimate of 147 °C/kbar given above using the superpositioning procedure. Several factors are responsible for the success of this shifting procedure. For the moderate pressure considered here, the scattering profiles are insensitive to the effects arising from compression of the unit scattering volume, given the typical melt compressibilities of polymers, ~1×10^{-3} $kbar^{-1}$. The dominant feature of the scattering from block copolymer melts near the LDOT or UODT arises from segregation effects.[1,2] In conventional UODT block copolymers, small-amplitude composition fluctuations with size scale ~R_g develop in the disordered state many tens of degrees above the transition.[3] In the case of the LDOT, these fluctuations in the disordered state appear to dominate the scattering behavior many tens of degrees below the transition regardless of the external pressure. As a result, high pressure SANS profiles closely

resemble those at low pressures within the temperature range of these experiments. A simple linear shift of temperature in the peak parameters plots will therefore closely reproduce the pressure coefficient.

In cyclic pressure sweeps, hysteretic behavior was noted in the ordering and disordering throughout these experiments. The arrows in Figure 2.9 show the direction of the pressure sweep. At 140 °C, disordering occurs at 276 bar with increasing pressure, while with decreasing pressure reordering occurs at 206 bar, a difference of ~70 bar. At 160 °C, the hysteresis is ~40 bar. Since an independent measurement showed that the ordering time was more rapid than the experimental detection time, a detection lag was eliminated as a cause of the observed hysteresis. This apparent stabilization of the ordered state with respect to the disordered state could be explained either by the metastibility of the disordered state as pressure is decreased or by the tendency for increased stability of the ordered state over time, as grain structure continue to perfect during extended annealing. Grain size and perfection has recently been observed to have minor effects (~1.5 °C) on the transition temperature in thermal studies of the UDOT.[4]

C. Phase Diagram

A coarse-grained T-p phase diagram was constructed based on the results of the SANS measurements for all molecular weights, as shown in Figure 2.10. The ordered and disordered states were identified based on observed discontinuities in the peak parameters. In this diagram, the LDOT was defined as the temperature halfway between the two temperatures where the discontinuity was observed. For the

experimental resolution of 12 °C and 170 bar, these transition lines, therefore, have uncertainties of at least 6 °C and 85 bar. The phase diagram shows clearly the strong effect of pressure on the LDOT for all the molecular weights investigated. The slope of the LDOT lines from this phase diagram are estimated to be in excess of +125 °C/kbar, independent of molecular weight. Recent measurements of the pressure coefficient in UODT block copolymers have not been observed to exceed ~20 °C/kbar. Implications of the sharp increase in dT_{LDOT}/dP are discussed further below. At this experimental resolution, no systematic dependence of the slope on molecular weight can be detected.

D. Summary

In these studies, a quantitative examination of the pressure dependence of the LDOT of p(*d*-S-*b*-nBMA) block copolymers has been presented. For the four molecular weights investigated, the pressure coefficient exceeds 125 °C/kbar. This value is greater than current observations in UODT block copolymers by a factor of five. The dramatic slope of the LDOT line in the T-p phase diagram allows rapid access to the disordered state by application of pressure, even in cases where the transition is kinetically inaccessible due to glass formation. Since block copolymers are often used as compatibilizers or interfacial modifiers, the materials studied here could be usefully exploited to impart pressure-induced compatibilization, enhanced surface activity, or new flow properties to blend or multicomponent systems. The p(S-*b*-nBMA) appears to be, in general, an especially robust system, since the transition temperature and

pressure are tunable over hundreds of degrees via small differences of the total molecular weight and the relative fraction of the block length.

New experiments are suggested by the observation of the dramatic slope of the LDOT phase transition line. As discussed in the following chapter, the slope is controlled by both the entropy and volume changes across the transition. It is of interest to examine closely these measurable quantities and make contact with recent observations obtained for block copolymers with UODT phase behavior. An analysis of the thermodynamics of these UODT and LDOT systems is discussed in Chapter 4.

E. References

[1]Theory of microphase separation in block copolymers. Leibler, L. *Macro.* **1980**, *13*, 1602.

[2]Fluctuation effects in the theory of microphase separation in block copolymers. Fredrickson, G. H.; Helfand, E. *J. Chem. Phys.* **1987**, *87*, 697.

[3]Block copolymers near the microphase separation transition. 3. Small-angle neutron scattering study of the homogeneous melt state. Bates, F.; Hartney, M. *Macro.*, **1985**, *18*, 2478.

[4]Equilibrium order-to-disorder transition temperature in block copolymers. Floudas, G.; Hadjichristidis, N.; Iatrou, H.; Pakula, T.; Fischer, E. W. *Macro.* **1994**, *27*, 7735.

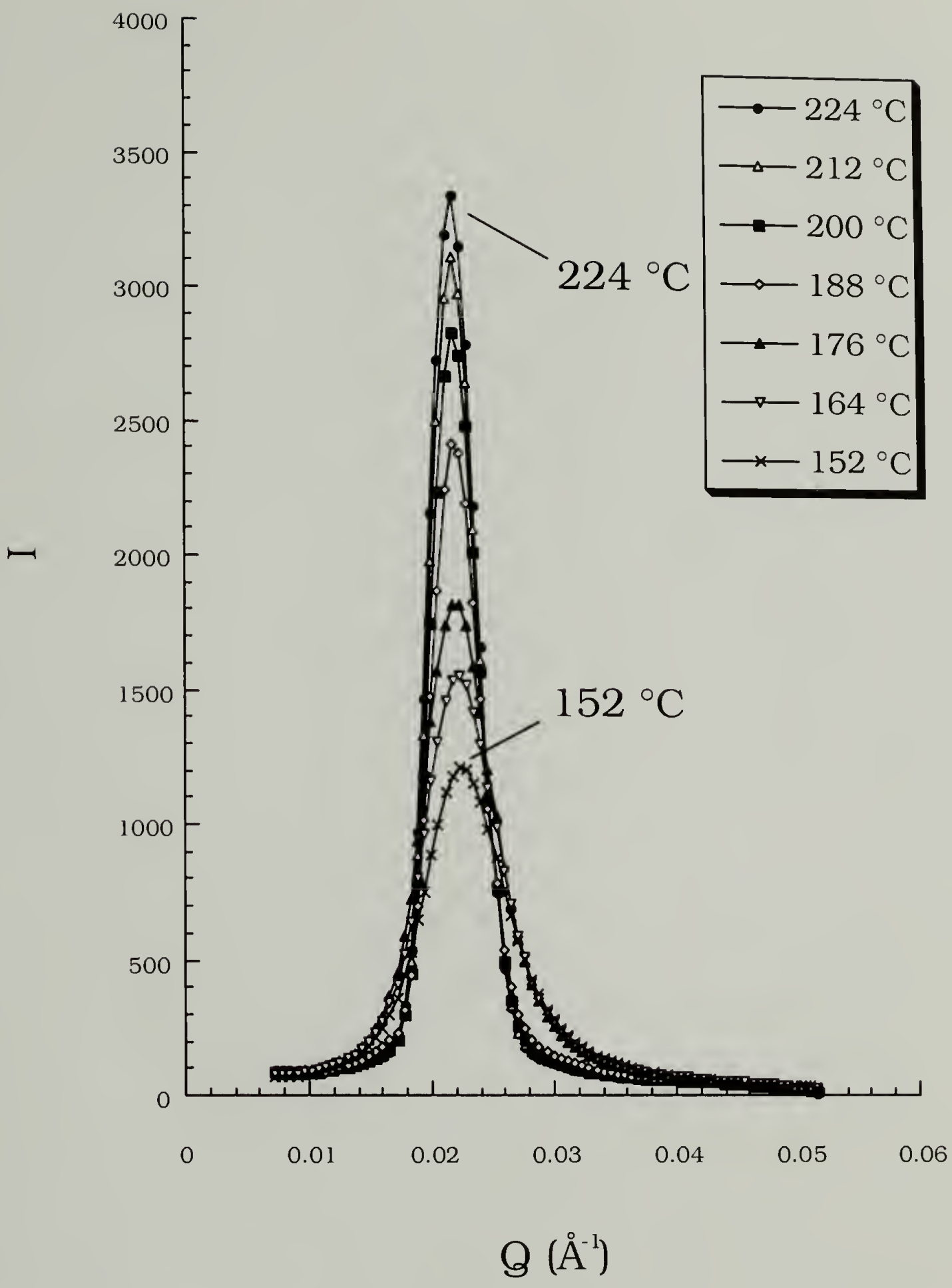

Figure 2.1 SANS profiles, 85k. I vs. Q ($Å^{-1}$), for p(*d*-S-*b*-nBMA). The discontinuous changes in peak shape between 176 and 188 °C pinpoints the thermal transition from the disordered to the ordered state.

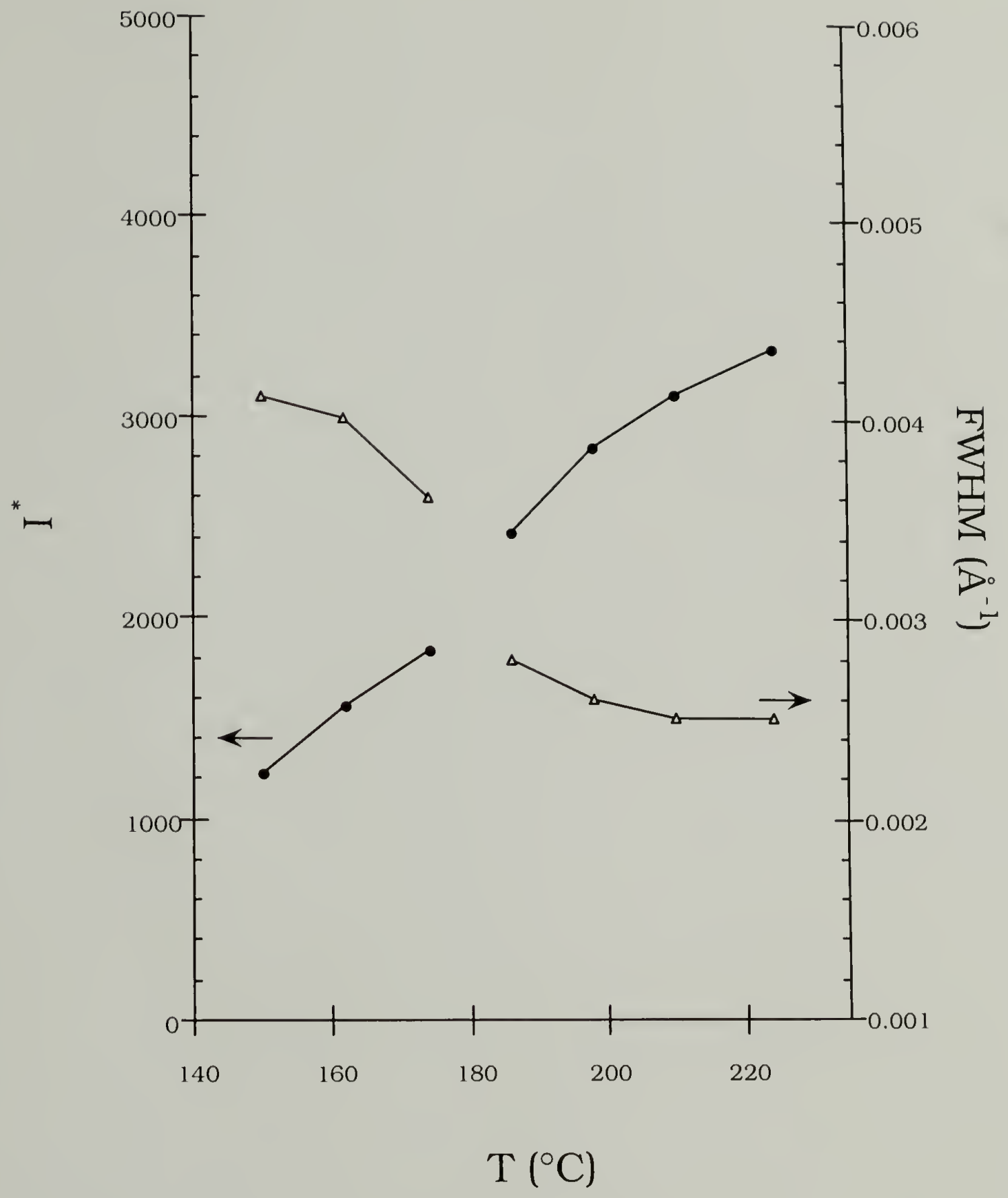

Figure 2.2 Peak parameters, 85k. Peak height and width as a function of temperature obtained from the SANS data in Figure 2.1. The discontinuity in these parameters are clearly observed at ~180 °C.

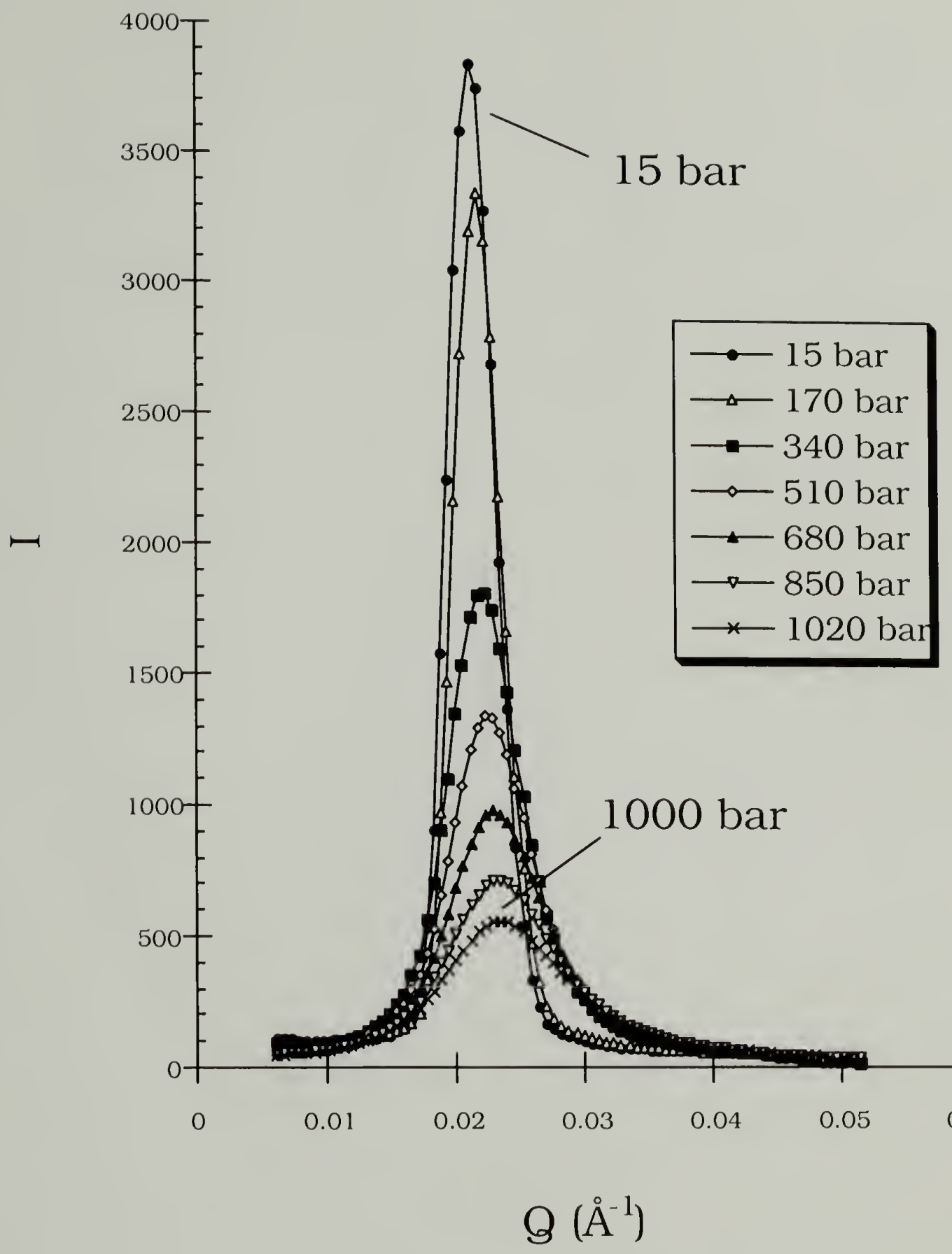

Figure 2.3 SANS profiles, 85k. I vs. Q (Å^{-1}), for 85k p(*d*-S-*b*-nBMA) at 170 °C. The discontinuous change in peak shape between 340 and 510 bar indicates the isothermal transition from the ordered to the disordered state.

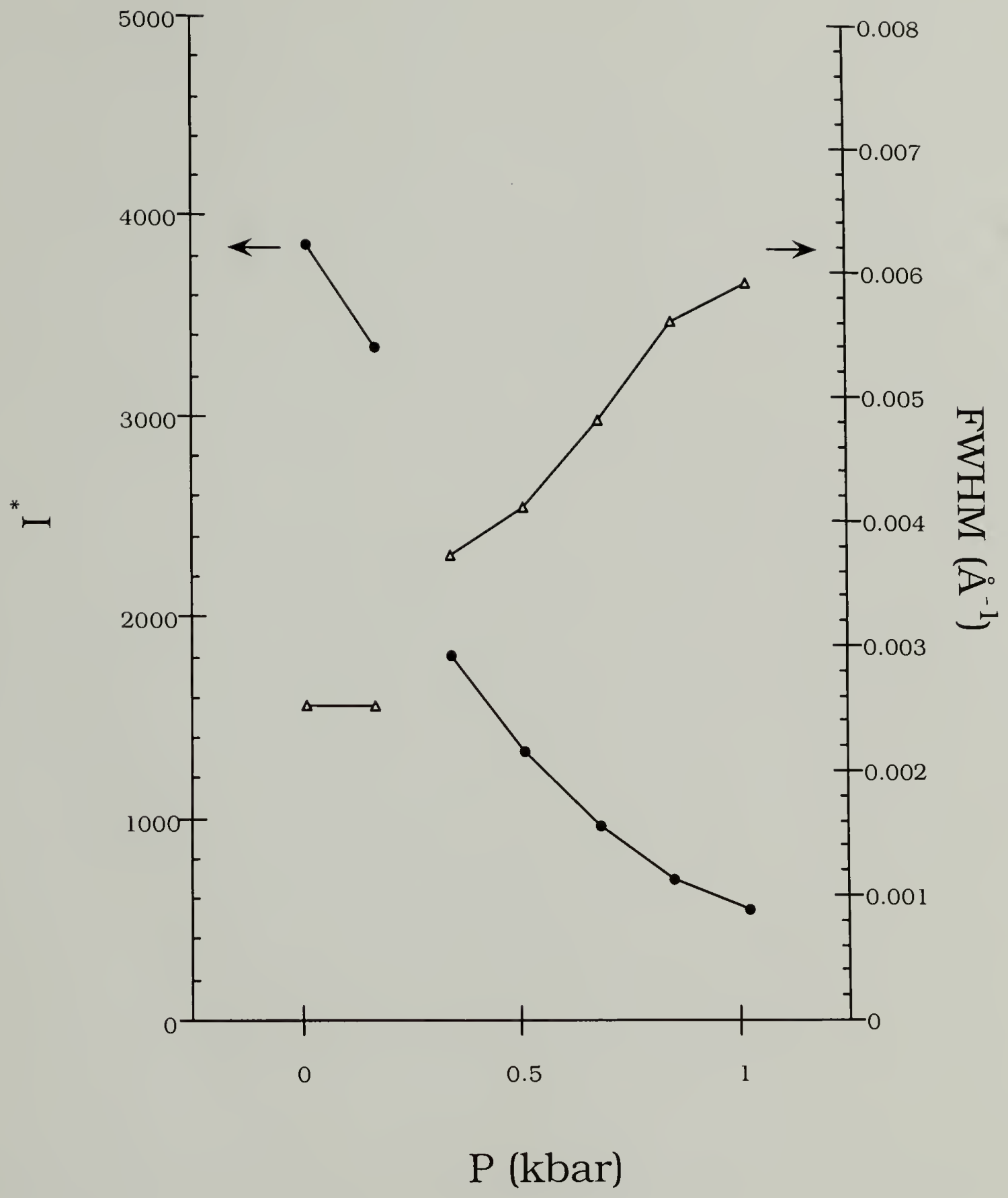

Figure 2.4 Peak parameters, 85k. Peak height and width as a function of pressure obtained from the SANS data in Figure 2.3. The discontinuity in these parameters clearly show the pressure-induced transition at ~250 bar.

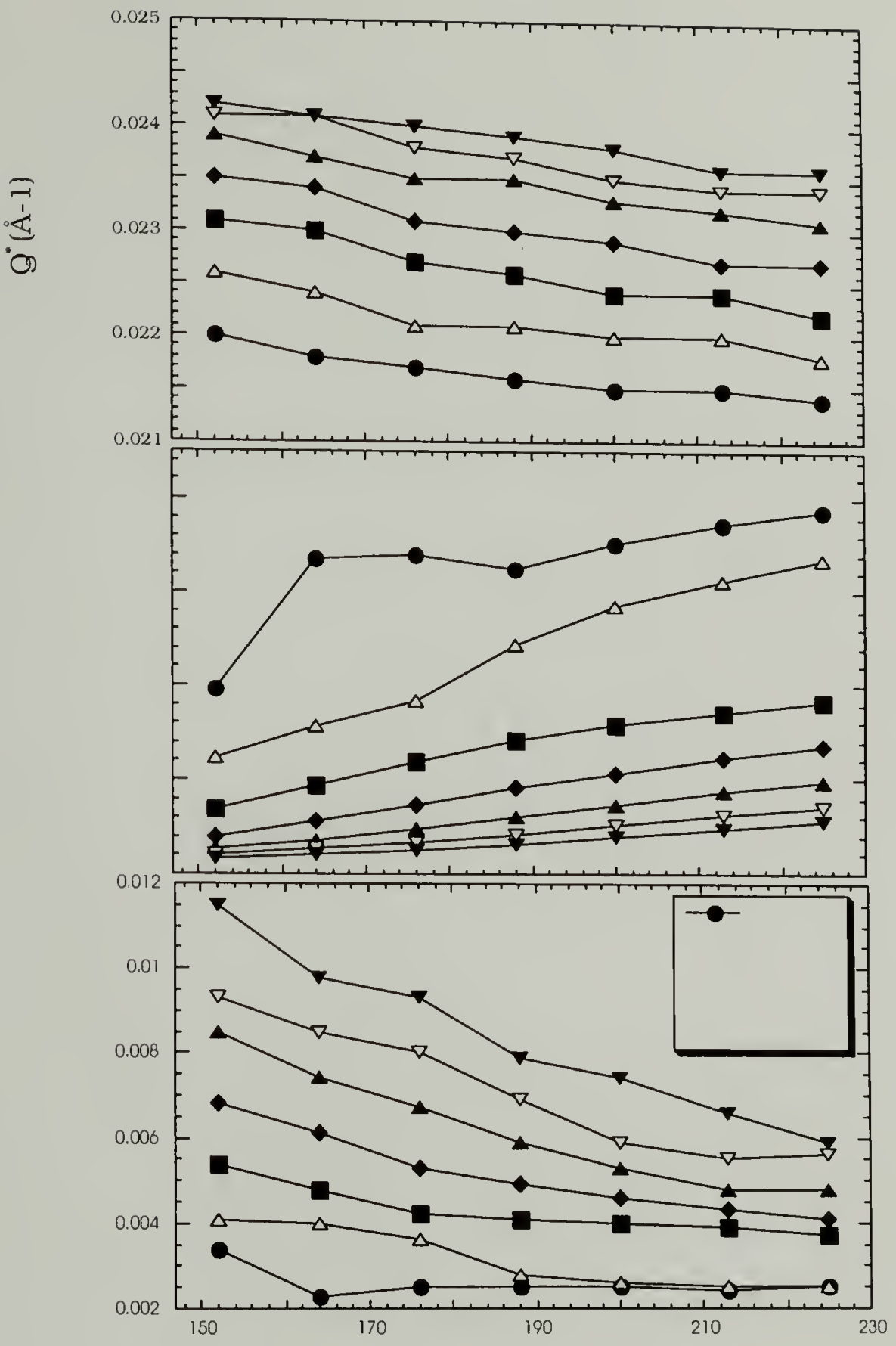

Figure 2.5 Peak parameters, summary. Obtained for the 85k p(*d*-S-*b*-nBMA) as a function of temperature and pressure. Transitions between the ordered and disordered regions are indicated by the dashed lines, which show that higher pressures produce a dramatic shift of the transition to higher pressure.

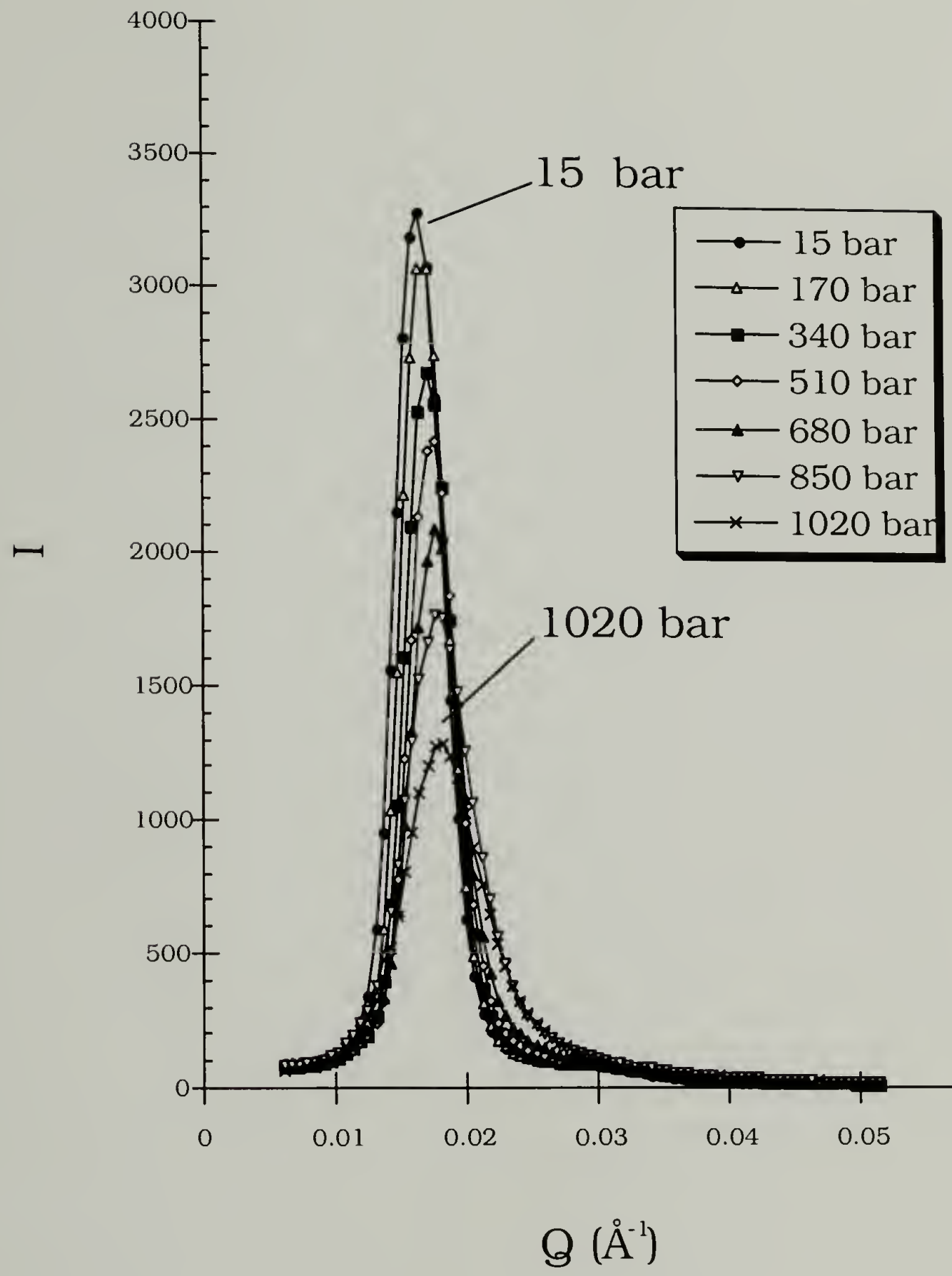

Figure 2.6 SANS profiles, 134k. I vs. Q ($Å^{-1}$), for p(*d*-S-*b*-nBMA) at 170 °C. The cylindrical morphology present at ambient pressure is disordered at ~700 bar.

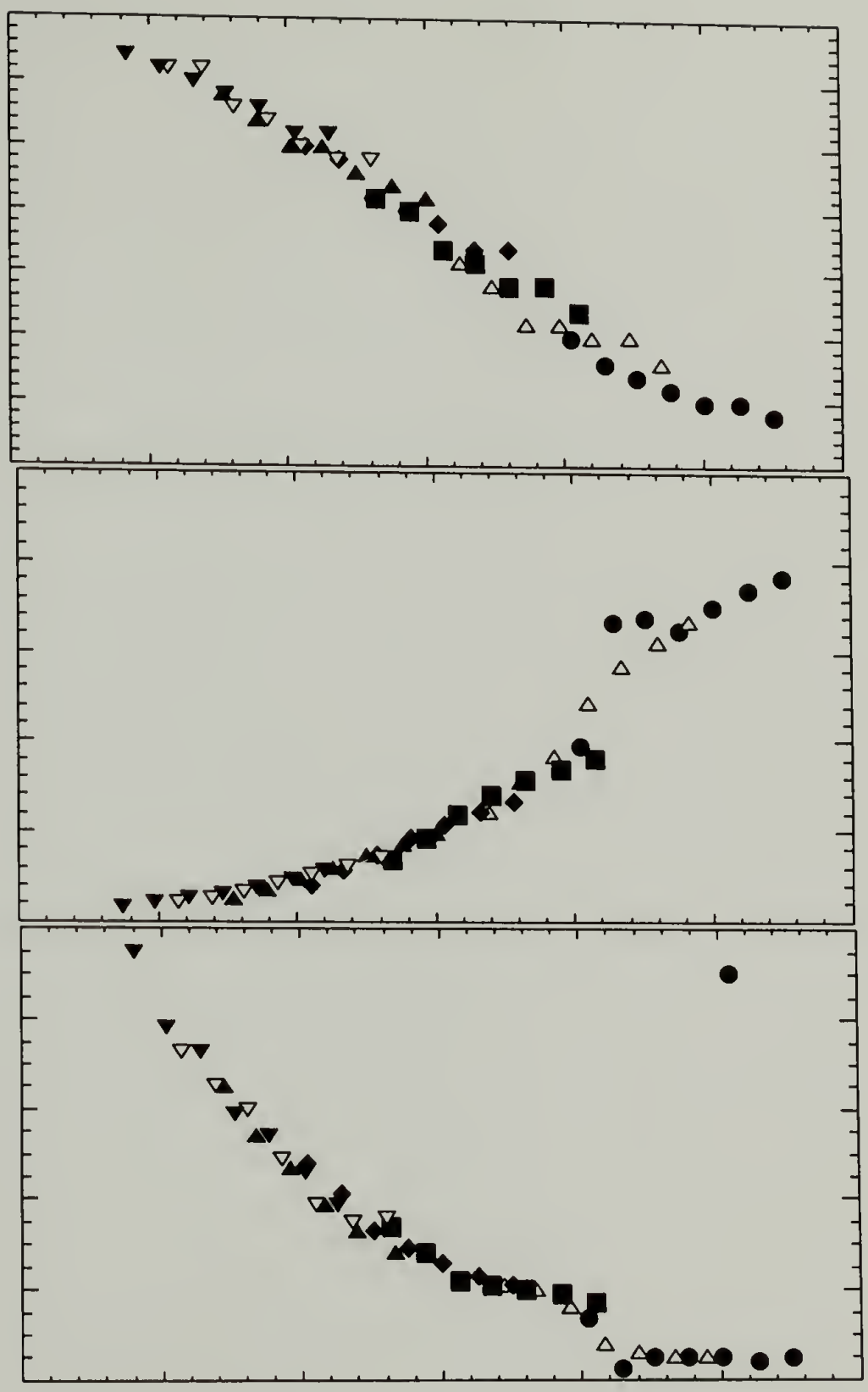

Figure 2.7 Temperature-pressure superposition, 85k. Significant overalp is observed by shifting the peak width (FWHM), peak height (I*), and wavevector at peak (Q*) along the temperature axis to the left by an amount proportional to the pressure.

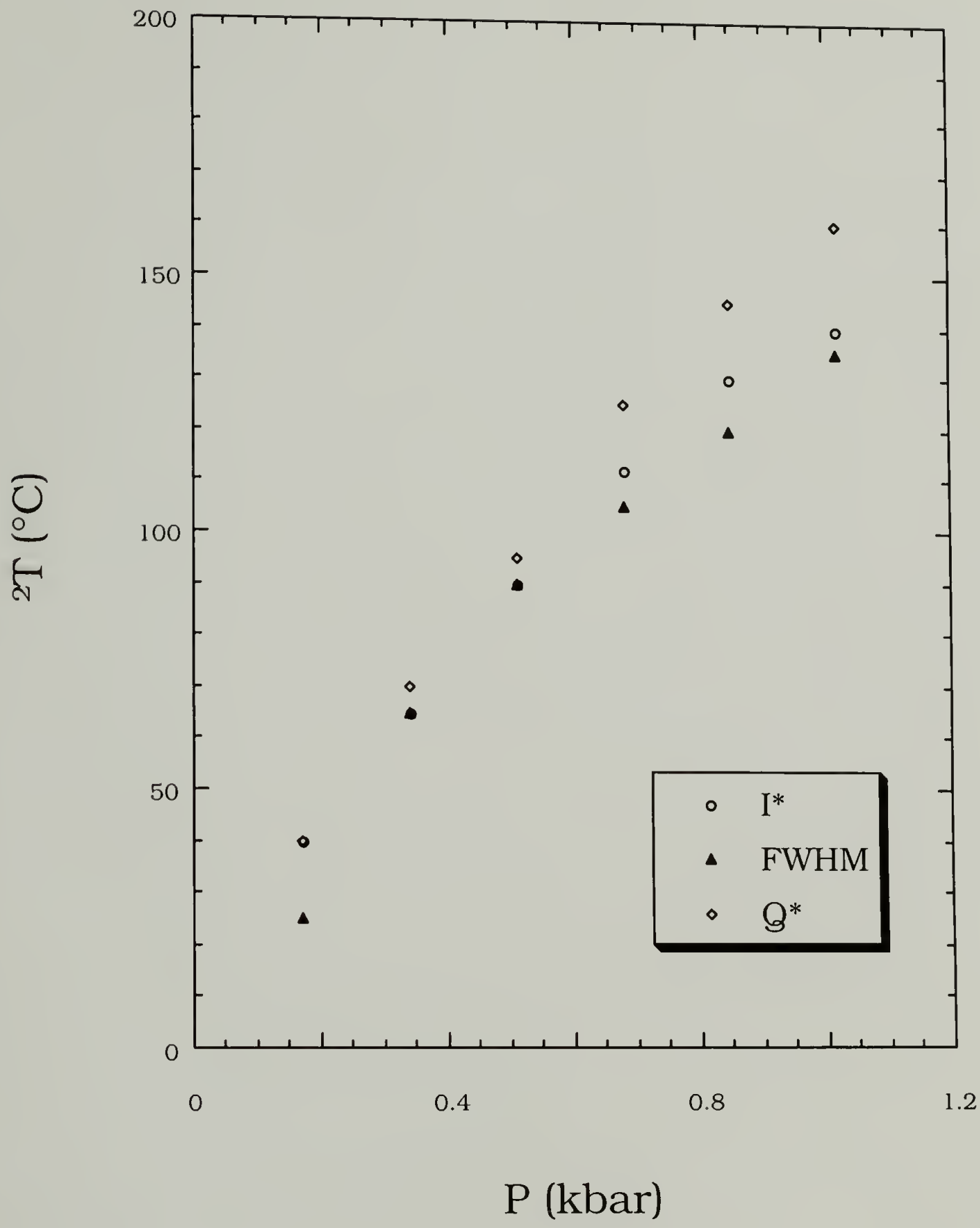

Figure 2.8 Pressure coefficient, 85k. Plot of shift temperature, ΔT, vs. pressure for the data shown in Figure 2.7. The amount by which data points were shifted corresponds to the pressure coefficient of the LDOT. At 1 kbar, a shift of ~130–150 °C is observed.

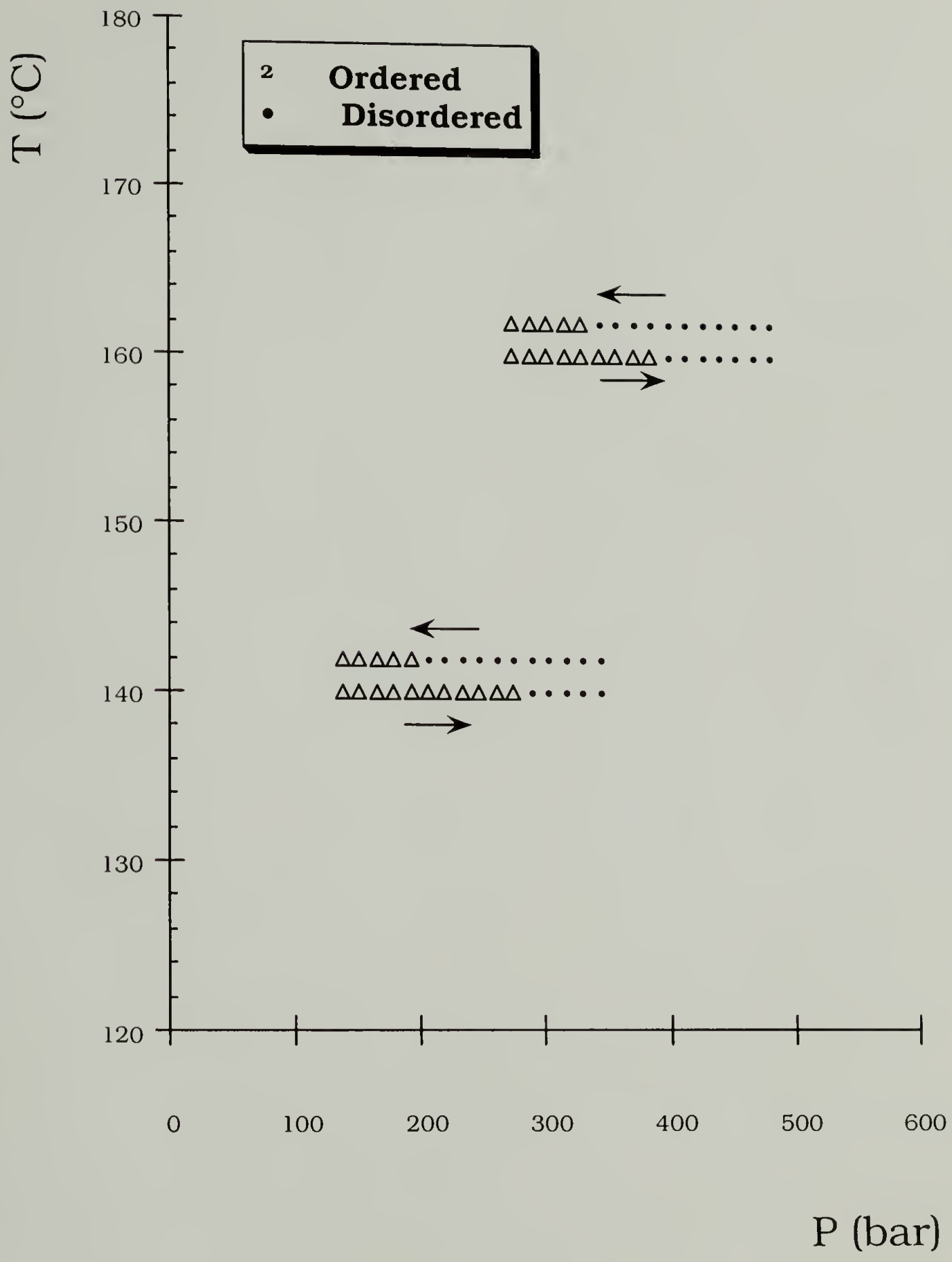

Figure 2.9 Phase diagram, 96k. Obtained for p(*d*-S-*b*-nBMA) using SANS wtih fine pressure increments. Hysteresis is observed upon ordering and disordering isothermally at 140 and 170 °C.

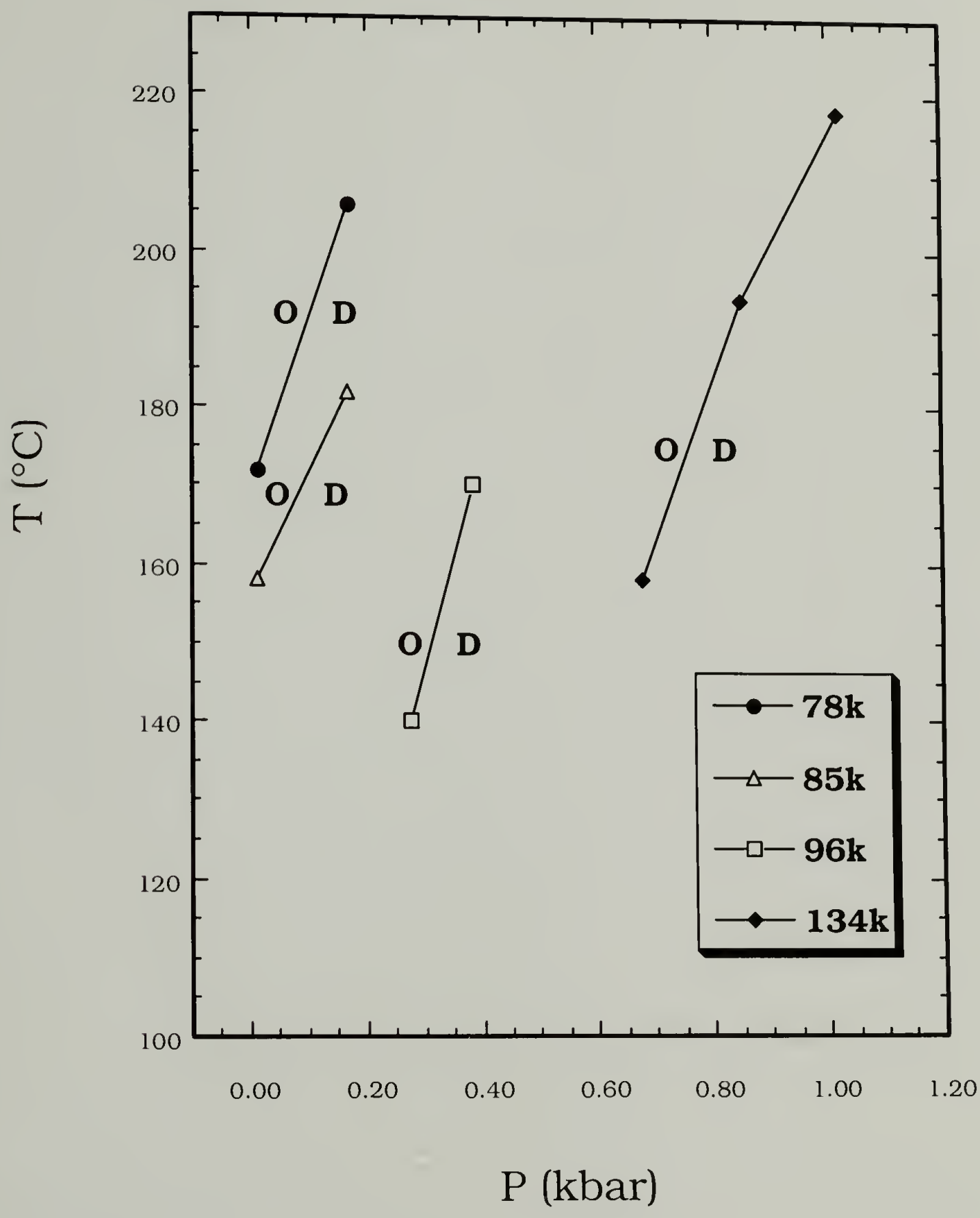

Figure 2.10 Phase diagram, summary. Shown are the LDOT lines for 78k, 85k, 96k, and 134k p(*d*-S-*b*-nBMA) obtained using SANS. Dramatic slopes, ~150 K/kbar, are observed for all molecular weights.

CHAPTER 3

VOLUME AND HEAT EFFECTS

A. X-Ray Reflectivity

Objective. Neutron and x-ray reflectivity are scattering techniques that probe the structure and dynamics of thin films (~1–100 nm). A well collimated incident beam impinges upon the substrate-supported film at very low angles of incidence (~1–3°), and the fraction of beam intensity reflected specularly from the substrate is monitored as a function of the incidence angle. A number of parameters of interest can be obtained by fitting the reflectivity curve, R vs. Q, to a model of the film's density profile in the z-direction, using the Parrat formalism.[1] Reflectivity, R, is the ratio of the (constant) incident intensity to that reflected into a given angle, and the wavevector is defined by $Q=(4\pi/\lambda)\cdot\sin(\theta)$, where θ is the impingement angle. The film thickness in particular produces a characteristic pattern of minima and maxima, known as Kiessig fringes, which result from interference between the radiation reflected from the substrate-film interface and from the film-air interface. Iterative fitting of the fringe pattern in the reflectivity curve using this model yields a precise measurement of the film thickness.[1] Neutron reflectivity has also been used to measure the thermal expansion coefficient of thin homopolymer films.

We are interested in using x-ray reflectivity to obtain indirect information on the bulk volume change expected to occur at the LDOT in p(*d*-S-*b*-nBMA). By measuring the film thickness of p(d-S-b-nBMA) as a function of temperature, the volume

expansion expected at the LDOT will be reflected as a discontinuous change in the sample thickness. This gives an estimate of the bulk ΔV_{ord} expected for this system.

Experimental. X-ray reflectivity measurements were performed on a Rigaku RU-300 rotating-anode instrument. This instrument is currently configured with a copper anode target and two orthogonal exit windows, one for point source illumination and one for line source illumination. The point source is used for traditional small-angle x-ray scattering (SAXS), and the line source for x-ray reflectivity (XR). The reflectometer is a home-built instrument consisting of a Si crystal monochromator, manually adjustable slit micrometers, and solid-state detectors. Sample mount and detector rotation angles are controlled by stepping motors with an accuracy of 0.01°. Samples on channel-cut Si wafers are locked into a sample mount which allows temperature control from 35 °C to 200 °C, and transparent Kapton entrance and exit windows on the chamber allow operation under vacuum. A beam monitor, which consists of a detector placed orthogonal to the beam line and a Kapton window that reflects a small portion of the beam into the detector, is used to monitor the condition of the collimation and configuration of the instrument, which require periodic adjustment. A DOS computer program controls the motors and collects data exiting the pulse-height discrimination array using a user-edited set of macros. Due to the limited range of linearity in the detector, foils of aluminum are placed between the sample and the detector to limit the beam intensity to the range 1 000 – 10 000 cps. Reconstruction of the reflectivity curve requires scaling the intensity based on the number of foils present (10 foils ~ 1/10 I_o). Since no absolute intensity monitor is available, unit reflectivity is arbitrarily assumed to be that observed below the critical angle.

The 85k p(*d*-S-*b*-nBMA, with LDOT = 155 °C, was chosen for the initial studies of film thickness versus temperature. Thin films were spin-coated from ~5 wt% toluene solutions onto Si wafers, resulting in initial film thicknesses in the range 230–260 nm. Experiments were conducted in three, four, or five degree increments from 130 to 170 °C. The reflectivity curve for each temperature consisted of the average of three complete θ/2θ scans, where θ is the grazing angle of incidence, from θ = 0.15 to 1.5°. Counting times for each scan ranged from one second at low θ to five seconds at high θ, with total acquisition of three scans requiring ~1 hr per set temperature. Approximately 3 days was therefore required to complete the experiment for one sample. Thermal expansion of the substrate was accounted for by realigning the sample before each new temperature. Each collected scan was fit to a three layer model consisting of Si, SiOx, and the polymer using the Parrat formalism, with sample thickness an adjustable parameter.

Results. Figure 3.1 shows a selection of reflectivity curves obtained at four temperatures which span the expected bulk LDOT for the 85k p(d-S-b-nBMA). These curves, which have been offset vertically for clarity, show the typical features of reflectivity curves for thin polymer films. Unit reflectivity is observed below the critical wavevector, Q_c, of Si (~0.016 $Å^{-1}$), where the x-rays are totally externally reflected. Absorption and intererence effects due to the film thickness are observed above the critical wavevector, where the reflectivity drops as $R \sim Q^{-4}$. The periodic minima (Kiessig fringes) arising from the interference of radiation reflected specularly from the polymer/air interface and from the substrate/polymer interface can be used to calculate the film thickness, since $t = 2\pi/\Delta Q$. A value of 2650 Å is obtained by using

5 fringes at high wavevector. However, much better resolution is obtained by fitting to the three layer model, in which ~0.3% variation in the thickness parameter results in ~10% variation of $<\chi^2>$. As shown by the solid line fits to the discrete data points, a discontinuous change in the fringe width can be observed at ~149 °C.

The full data set is summarized Figure 3.2, where the best-fit film thickness is shown as a function of the temperature. Despite the large errors associated with the averaging of data sets, the LDOT can be identified at ~149 °C where both a change in slope and discontinuity are observed. Expansion coefficients of the thin film above and below this transition temperature are estimated from best fit lines through the data, which give $\alpha_{dis} \sim 0.9$ Å/K and $\alpha_{ord} \sim 2.1$ Å/K. The coefficients of expansion are therefore $\alpha_{dis} \sim 3.8 \times 10^{-4}$ K^{-1} and $\alpha_{ord} \sim 8.6 \times 10^{-4}$ K^{-1} with a difference $\Delta\alpha \sim 4.7 \times 10^{-4}$ K^{-1}. The thickness discontinuity is estimated by the extrapolation of the two best fit lines to the transition temperature, which gives $\Delta t \sim 7$ Å, or $\Delta t/t \sim 0.3\%$.

B. Differential Scanning Calorimetry

Objective. The microphase separation transition is a weakly first-order phase transition, and for experimentally accessible transitions a latent heat is expected to occur as the transition is crossed. DSC has been used in several instances to measure the enthalpy change at the UODT, using block copolymers such PS-PI which disorder at accessible temperatures, and these typically have low molecular weights. Using available calorimetric methods, we would like to investigate the latent heat associated with the LDOT in p(d-S-b-nBMA) block copolymers. Kinetic factors are expected to be important in this case, since the LDOT materials have much higher molecular weights,

and due to the inverted temperature behavior, the scanning experiment will measure an ordering process, which is expected to be slower than disordering for lamellar morphologies.

Experimental. The calorimetry experiments were conducted on either a Perkin Elmer DSC-7 or Pyris instrument. The former instrument can be either ice-water or air-cooled, while the latter instrument features a liquid nitrogen cooling attachment. Both are power-compensation DSCs with high sensitivity and low noise (~20 μW peak-to-peak noise). Additional experiments were attempted on a Thermal Analysts (DuPont) DSC, a heat flux instrument with lower sensitivity. Due to the slow kinetics of ordering and the extremely low heat flow expected, a variety of isothermal and scanning techniques were applied to measure the endotherms. The materials chosen for study included molecular weights of 68k, 75k, 78k, and 85k, which have ordering temperatures between 150 to 225 °C. Sample preparation consisted of direct annealing of powder in the aluminum sample pans, casting from dilute solution into the pan, or melt pressing into small circular discs. Both non-hermetic and hermetic pans were used, and scan rates ranged from 5 to 40 °C/min. Plots are shown as differential heat flow (mJ/sec) versus temperature (°C).

Additional measurements were undertaken to determine the heat capacity, C_p, of a variety of p(*d*-S-*b*-nBMA) block copolymers and homopolymers of dPS, PS, and PnBMA. Samples were first carefully weighed, annealed under vaccum for ~ 12 hr, and reweighed, with typical losses of 0.5 mg in volatiles, and probable errors of ±0.5 mg. This is the greatest source of error in these measurements. The PE DSC-2 instrument was used with water cooling and argon purge gas. The measurement

technique followed that of Richardson, which is an isothermal-scanning-isothermal technique. Samples were first isothermed for 2 min at 90 °C to a constant baseline, then scanned at 10 °C/min to 120 °C, and then isothermed for 2 min at 120 °C to a constant baseline. This procedure was then repeated in the ranges 120-150 °C, and 150-180 °C. Both an empty pan and a sapphire standard were run under identical conditions, and an empty pan was always used in the second (reference) crucible. Data reduction consisted of subtraction of the empty pan signal from the sample signals and multiplication by the calibration constant. For ease of comparison and calculation, 145 °C was chosen as a reference temperature.

Results. Typical results are shown in Figure 3.3, where the differential heat flow (mJ/s) is shown versus temperature for scans of three identically prepared samples. Curvature is due to an arbitrary slope correction. An endotherm is expected at ~180 °C for this 75k material. The thermal event recorded at 190 °C cannot be assigned with confidence to the phase transition due to high background noise (S/N ~ 4) and the lack of reproducibility in the two additional scans. At the magnification considered here, spurious changes in the baseline and poor reproducibility can be caused by sample delamination or dewetting, the escape of air bubbles, or sample flow.

Additional experiments using a variety of scan rates and sample preparations were unsuccessful at reproducing the heat flow associated with the LDOT or showing any heat capacity difference between the disordered and ordered states. The most probable reason for this difficulty is a combination of the low expected enthalpy change (< 0.1 mJ/mg) and the kinetic dominance of the phase transition. Calorimetry experiments are typically limited to a range of scan rates: 20 °C/min is the fastest rate

achievable without appreciable thermal lag, and 5 °C/min is the slowest, due to the loss of signal-to-noise (with peak-to-peak noise of 0.02 mJ/sec, a 1.0 mJ transition requiring 10 sec corresponds to S/N ~ 5). For a phase transition at 170 °C and sample decomposition at 220 °C, this corresponds to an experimental time range of 10 min at the fastest rate, and 2.5 min at the slowest rate. Additional factors that may be significant in this case include the metastability of the disordered state, i.e. superheating, and the finite induction time required for the growth of the ordered phase. Significant quenches (~10 °C) into the metastable region above the transition will be required to nucleate the new ordered phase at an observable rate.

These results suggest that further experiments must be conducted. An optimized heating measurement should take into account the kinetics of both local microphase separation and the growth of ordered domains to impingement, and how these processes are affected by a linear heating ramp. For full optimization, material parameters such as viscosity, molecular weight, and ordering temperature must be balanced with the allowed heating rates. A cooling experiment is an additional option that should be fully explored, since nucleation and growth are not required when disordering or melting. The rate of this process, by contrast, will be much faster, as observed in the melting of polymer crystals, for example. However, in contrast to the UODT, disordering by cooling will increase the viscosity, and it will be necessary to choose a material with an optimal ordering temperature and a sufficiently slow cooling rate.

C. Polarized Light Microscopy

In view of the kinetic factors that may complicate the transition enthalpy determination, a preliminary series of microscopy experiments was carried out to estimate approximate ordering times when quenched thermally into the ordered state. Balsara pioneered the use of polarized light microscopy and light scattering to study in detail the ordering transition in block copolymer melts.[7] In a lamellar diblock copolymer, the periodic density fluctuations in the ordered state give rise to a form birefringence.[8] Domains of lamellar or cylindrical structures exceeding ~10 microns in size will depolarize incident polarized light (unless viewed down the optic axis), and can therefore transmit light under crossed-polar conditions. They are typically viewed as bright regions in a dark field.

To roughly gauge the characteristic ordering times of these block copolymers, the quench depth, $T\text{-}T_{LDOT}$, was varied in-situ using a hot stage with separate samples (~0.1 mg) pre-annealed on glass slides. Observation of the onset of ordering was determined by eye, and quench temperatures were set from 190 to 230 °C, covering the entire time range accessible (10 sec – 30 min). The results are shown in Figure 3.4, where the onset time is shown versus the quench temperature. Bulk LDOTs for the 75k and 78k p(*d*-S-*b*-nBMA) are ~163 and ~180 °C. A linear relation between the temperature (or quench depth ΔT) and $\log(t_{onset})$ is observed over the entire range of quench temperatures. The extreme sensitivity to temperature of this characteristic ordering time indicates that more effective calorimetric measurements will require much finer increments in the scan rate than have been employed in the experiments conducted above.

D. Discussion

The results obtained from these experiments are a first effort towards capturing the equation of state effects associated with the LDOT in block copolymers. One mixing property that features strongly in LCST blends, but has not been studied extensively due to experimental limitations, is the excess mixing volume. One gauge of this effect in the case of the LDOT is the observation above that the expansion coefficient for p(d-S-b-nBMA) in the disordered state is not a weighted-sum of the expansion coefficients for the parent homompolymers. The literature values for PS and PBMA are $\alpha_{PS} = 5.1 \times 10^{-4}\ K^{-1}$ and $\alpha_{PBMA} = 6.1 \times 10^{-4}\ K^{-1}$ at similar temperatures above T_g,[2] while the observed expansion coefficient in the disordered state, at $3.8 \times 10^{-4}\ K^{-1}$, is less than the weighted average of the two. This reduction by a factor of 1/3 may be attributed to a reduction in the free volume in the disordered state compared to pure PS or PBMA homopolymers.

Until recently very few studies have been devoted to understanding how asymmetric monomers pack locally and how this affects the thermodynamic mixing properties.[2-6] These considerations are crucial in designing polymer blend systems with specific morphologies, since the phase behavior depends sensitively on this type of local microstructure. As Balsara and Krishnamoorta have recently shown in blend studies of polyolefins, even simple structural changes exert profound effects on the blend thermodynamics, in particular the mixing behavior.[7] The unusual observations of poly(isobutylene) emphasize this point since, despite the presence only of van der Waals interactions, this system is an exception among polyolefins in forming a number

of miscible blends with other polyolefins, and appears to suffer a volume reduction upon mixing. Typical polyolefins show only UCST-type phase behavior and endothermal mixing. Although 'local packing effects' were invoked to explain this behavior, these are poorly understood effects and only empirical relations are used to describe the behavior.

Since the excess mixing volume in blends is controlled to a large extent by this local structure and packing, there should be no discernible difference in the mixing behavior between miscible PS/PBMA blends and the disordered-state PS-PBMA diblock copolymers. If we interpret the reflectivity results of $\alpha_{PS\text{-}PBMA}$ as implying a negative excess mixing in this sytem, then PS/PBMA blends are also expected to densify upon mixing. In view of the difficulties associated with measuring mixing volumes in blends, an alternative route is to examine the thermal expansion coefficient of the blend. Further reflectivity experiments in PS/PBMA blend systems should therefore show reduced thermal expansion coefficients compared to the pure homopolymers.

E. References

[1]Russell, T. *Mater. Sci. Rep.*, **1990**, *5*, 171.

[2]*Polymer Handbook, 3rd Ed.* Brandrup, J.; Immergut, E., Eds. Wiley, New York, **1989**.

[3]Chain-Packing effects in the thermodynamics of polymers. Londono, J.; Maranas, J.; Mondello, M.; Habenschuss, A.; Grest, G.; Debenedetti, P.; Graessley, W.; Kumar, S. *J. Polym. Sci., Polym. Phys.* **1998**, *36*, 3001.

[4]Regular and irregular mixing in blends of saturated hydrocarbons in polymers. Graessley, W.; Krishnamoorti, R.; Reichart, G.; Balsara, N.; Fetters, L.; Lohse, D. *Macro.*, **1995**, 1260.

[5]Thermodynamics of isotopic polymer mixtures: significance of local structural symmetry. Bates, F.; Muthukumar, M.; Wignall, G.; Fetters, L. *J. Chem. Phys.*, **1988**, *89*, 535.

[6]Effect of molecular structure on the thermodynamics of block copolymer melts. Lin, C, Jonnalagadda, S.; Kesani, P.; Dai, H.; Balsara, N. *Macro.*, **1994**, *27*, 7769.

[7]Anomalous mixing behavior of polyisobutylene with other polyolefins. Krishnamoorti, R.; Graessley, W.; Fetters, L.; Garner, R.; Lohse, D. *Macro.* **1995**, *28*, 1252.

[8]Birefringence detection of the order-to-disorder trnasition in block copolymer liquids. Balsara, N; Perahia, D.; Safinya, C.; Tirrell, M.; Lodge, T. *Macro.*, **1992**, *25*, 3896.

[9]The birefringence and mechanical properties of a 'single-crystal' from a three-block copolymer. Folkes, M.; Keller, A. *J. Polymer*, **1971**, *12*, 222.

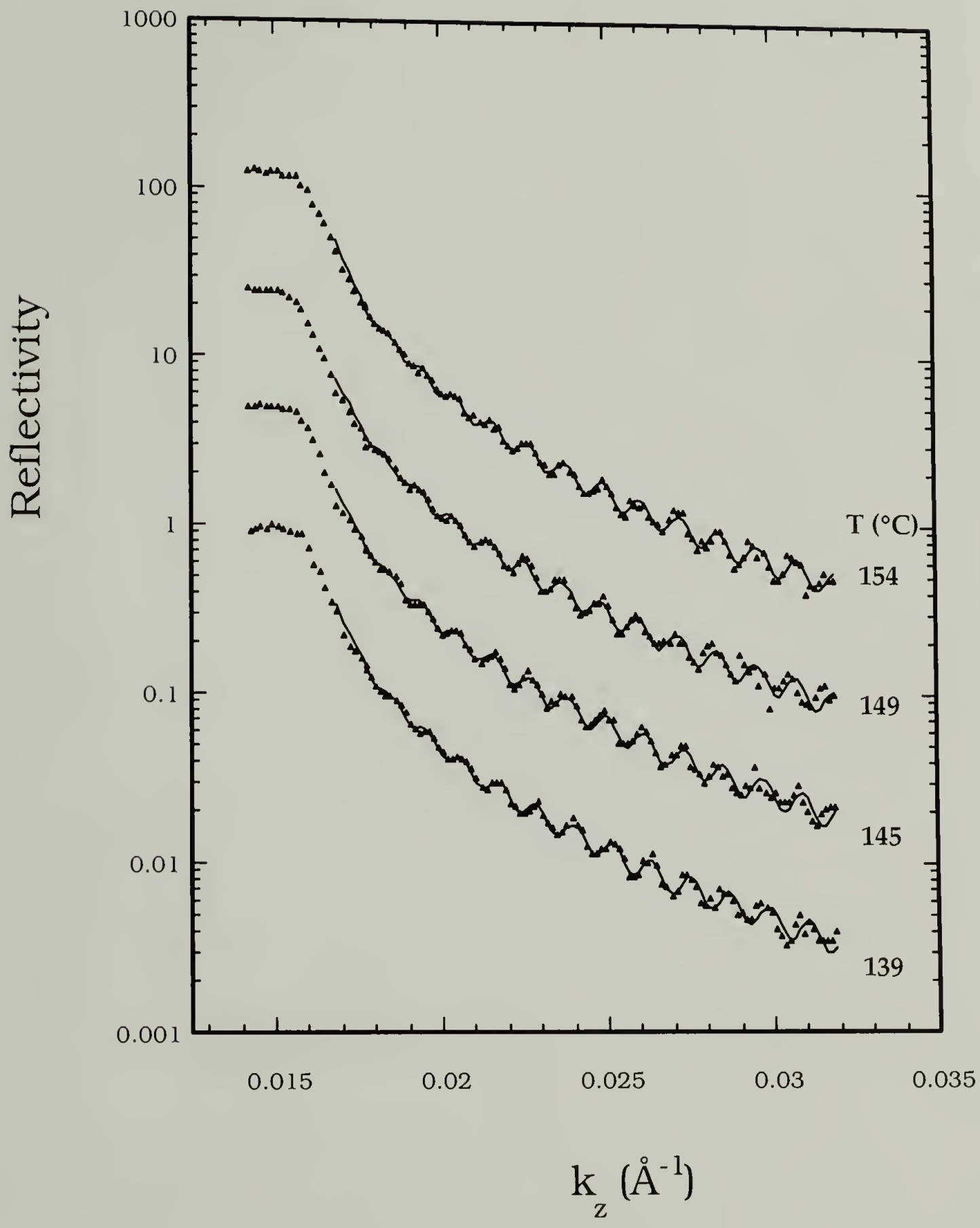

Figure 3.1 Reflectivity profiles, 85k. Selected profiles for 85k p(*d*-S-*b*-nBMA) as a function of temperature. Curves have been offset vertically for clarity.

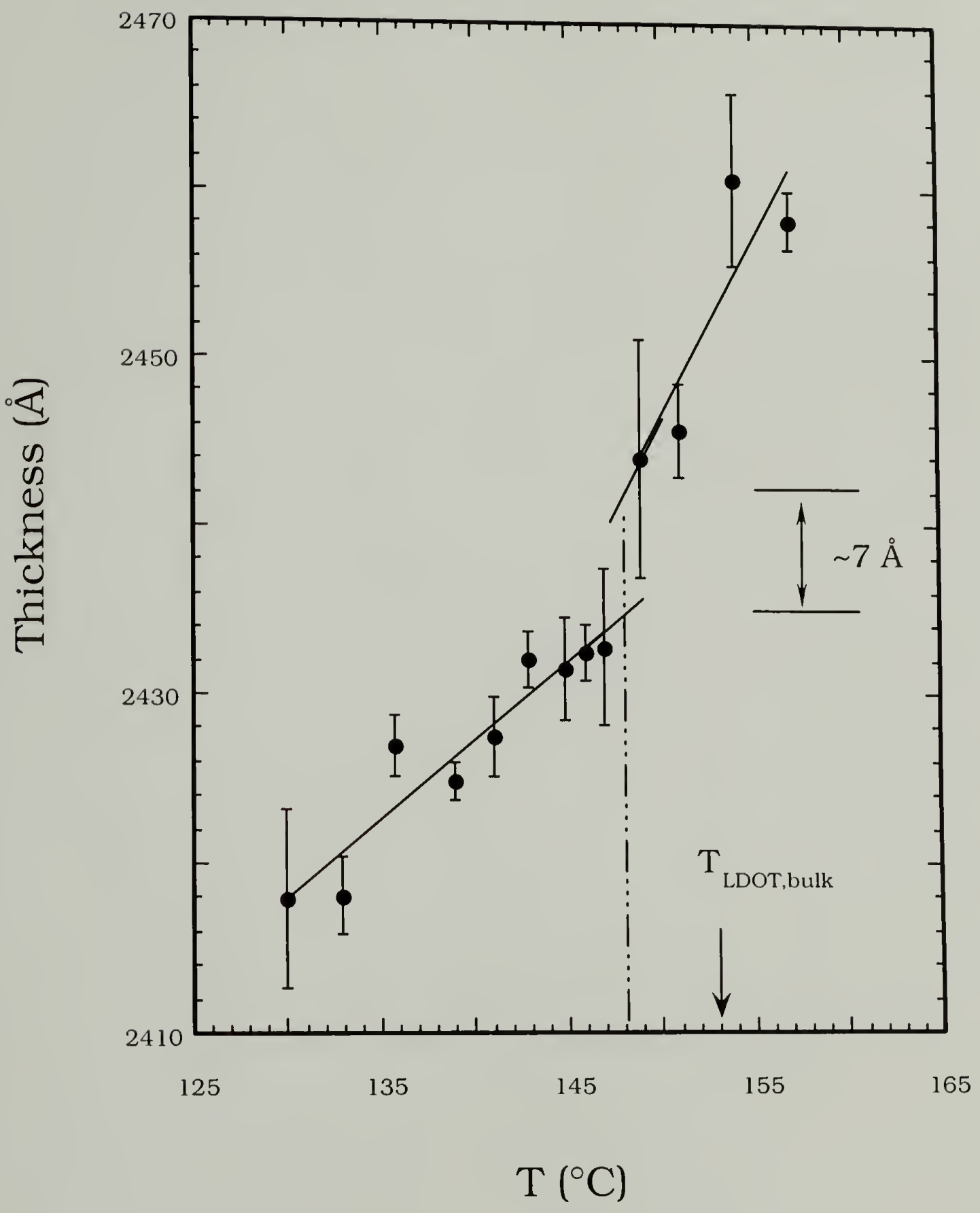

Figure 3.2 Film thickness discontinuity, 85k. Results obtained for 85k p(*d*-S-*b*-nBMA). An extrapolation of best-fit lines gives an estimate of the film thickness discontinuity at ~148 °C.

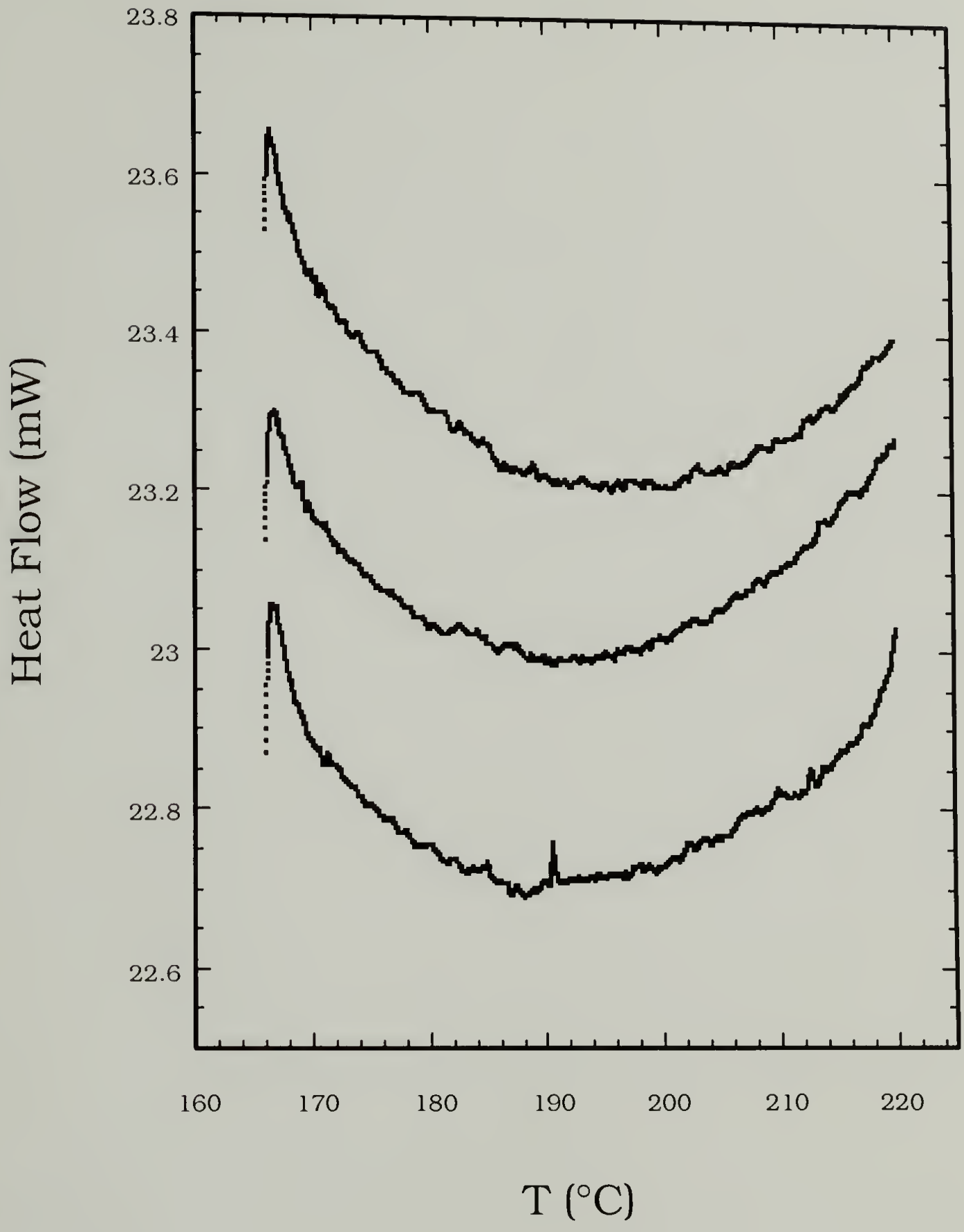

Figure 3.3 DSC, 75k. Traces obtained for 75k p(*d*-S-*b*-nBMA) at a scan rate of 5 °C/min. An arbitrary slope correction and vertical offsets have been applied. Unknown factors lead to poor reproducibility of the endotherm at 190 °C.

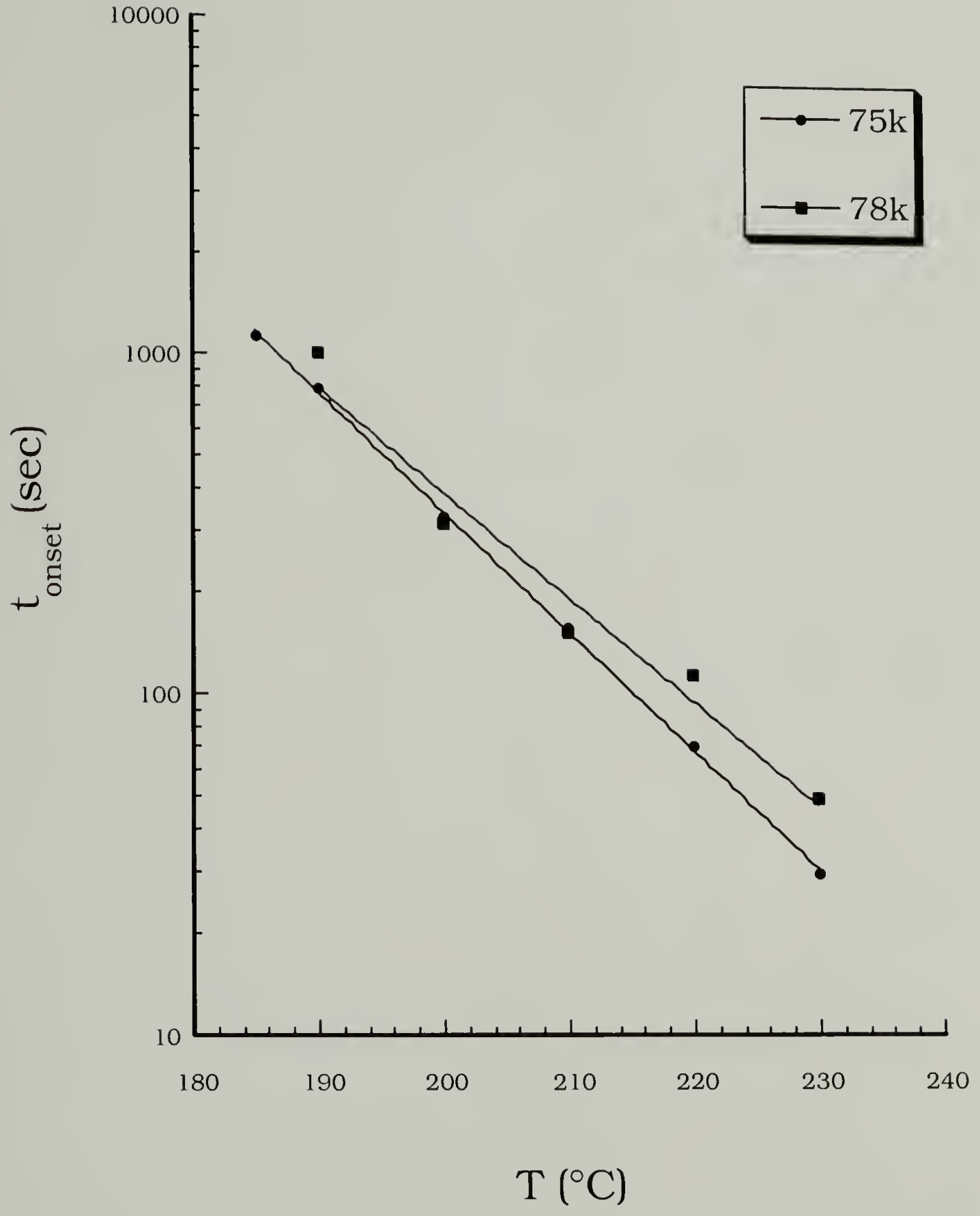

Figure 3.4 Ordering kinetics, 75k & 78k. Obtained for p(*d*-S-nBMA) by polarized light microscopy. A linear relation is observed between $\log(t_o)$ and the quench depth, ΔT.

CHAPTER 4

PHASE DIAGRAM OF p(*d*-S-*b*-nBMA)

A. Schematic Phase Diagrams

UODT. The T-P phase diagram expected for a one-component block copolymer with UODT phase behavior is shown schematically in Figure 4.1. It is assumed that both blocks contain noncrystallizable monomers and that the polydispersity in chain length is negligible. The dotted lines in the diagram indicate the thermal decomposition and the glass transition temperatures, which limit the accessible temperature and pressure range. The ordered and disordered states are equilibrium phases, and are labelled ORD and DIS in the diagram. The line extending outward from ambient pressure is the first-order UODT phase transition line. Its slope is controlled to a great extent by the average densities of the two phases at the transition. There are two possibilities:

(a) If the ordered phase is more dense ($\rho_{ord} > \rho_{dis}$), it will be favored at higher pressures, resulting in a transition line with a positive slope in the T-P plane. This behavior, observed in the solid-liquid coexistence line of the overwhelming majority of condensed materials, and is denoted (a) in Figure 4.1.

(b) If the ordered phase is *less* dense ($\rho_{ord} < \rho_{dis}$), it will be disfavored at higher pressures, resulting in a transition line with a negative slope of the ORD-DIS line in the T-P plane. This case occurs less commonly since higher temperature phases in general tend to be less dense; exceptions therefore require an expansion of the atomic structure upon ordering. A well known example is the solid-liquid coexistence line of H_2O, in

which the solid (ice) melts into a more dense liquid (water). This case, (b), is also shown in Figure 4.1.

As observed from the diagrams, a judicious choice of the temperature will allow experimental access to either a disordering transition or an ordering transition isothermally, by applying pressure. It can be anticipated that the isothermal transition becomes easier to access as the slope of the phase transition line, dT/dP, increases.

In rare cases, the slope of the transition line changes sign, resulting in a temperature extremum. This case is denoted (c) in Figure 4.1. Here, the ordered phase is less dense at low pressures, but becomes the more dense phase at higher pressures. This crossover is due to subtle changes in molecular packing as pressure increases. When the densities between the two phases are equivalent, the slope becomes zero. A example of this uncommon behavior is the solid-liquid coexistence line of carbon, which shows zero slope in the T-P plane at high pressures, where the density of solid graphite equals that of liquid carbon.

All three examples of the pressure dependence of the UODT have been observed experimentally. The first case is illustrated by Hajduk's result on block copolymers of poly(sytrene) and poly(isoprene), in which a positive rise of 20 °C/kbar was observed.[18] The second case was observed by Frielinghaus, who found a negative pressure coefficient of the same magnitude in block copolymers of poly(ethylenepropylene) and poly(ethylethylene).[21] Curvature of the UODT line was observed by Schwahn, who reported a coefficient of +15 °C/kbar for block copolymers of poly(ethylene propylene) and poly(dimethyl siloxane) at pressures above 1 kbar, and a negative coefficient at pressures below 0.5 kbar.[20] These trends in the response to pressure of the UODT transition line are typically ascribed to the two competing

effects. First, by forcing segments closer together, the application of pressure will increase the segmental interaction energy. This leads to a decrease of compatibility and gives rise to positive pressure coefficients. As noted above, this is the case in the majority of endothermic melting transitions such as the UODT. However, if there is a net contraction upon disordering, then the application of pressure will enhance miscibility at low pressures. This is observed in the case of poly(ethylenepropylene-*block*-ethylethylene), where the expected decrease of compatibility with pressure is not observed due to an unexpected contraction upon disordering (or, equivalently, expansion upon ordering).

LDOT. Although the phase diagram associated with the UODT has been explored carefully for two decades, the observation of the LDOT phase behavior in block copolymers was relatively recent. Thermally accessible LODTs were found in a limited range of molecular weights (~6–10 x 10^5 g/mol) block copolymers of deutered poly(styrene) and poly(n-butyl methacrylate), as shown by small-angle X-ray scattering. In these initial experiments, the molecular weight dependence of the transition temperature and the rheological properties were first established.[5] This provided a basis for further exploration of the phase diagram. Subsequent pressure-dependent SANS measurements, reported in Chapter 2, allowed the slope of the phase transition line to be determined, and molecular weight effects to be examined. The resulting LDOT phase diagram is shown in a schematic form in Figure 4.1 along with the conventional phase behavior discussed above. In addition to the inherent temperature inversion of the phases, the primary contrast between the two types of phase behavior is quantitative: the slope of the phase transition line is much greater

than any previously observed value. This robust behavior allows access to an order-disorder transition, isothermally, with much greater ease than previously available.

B. Experimental Studies

Pressure Studies in Diblock Copolymers. Hajduk was the first to study the role of pressure in the phase behavior of block copolymers in a systematic and careful manner. High-pressure SAXS was used to determine the UODT of PS-PI diblock copolymers as a function of pressure. The coefficient of 20 °C/kbar was consistent with measurements of the volume change, $\Delta V_{dis}/V$, of order 10^{-4}, and the calorimetrically determined enthalpy change, ΔH_{dis}, of order 0.1 J/g.[18] Stamm published an early report that the application of pressure forced diblock copolymers of poly(styrene) and poly(α-methyl styrene) to undergo a transition from the ordered to the disorded state. This implied that the UODT decreased with pressure for this system, but the coefficient was not quantified.[19]

In a careful SANS study of poly(ethylene-propylene-*block*-dimethyl siloxane) with symmetric block lengths, Schwahn observed first a decrease of the UODT with pressure for $P < 0.5$ kbar, followed by an increase of the UODT up to 1.5 kbar.[20] This unusual curvature was attributed to unusual changes of the entropic Flory-Huggins parameter as a function of pressure. This group also performed SANS measurements of diblock copolymers of poly(ethylene propylene) and poly(ethylethylene), where a reduction of the UODT with pressure was observed.[21] A minimum was also observed by Steinhoff in the phase transition curve of poly(styrene) and poly(isoprene)

copolymers at pressures below 6 bar, while at pressures above 6 bar the results of Hajduk were reproduced.[10]

Pressure Studies in Blends. Despite the distinct difference between the thermodynamics of two-component A/B blends and one-component A-B diblock copolymers, they often have similar pressure behavior. The literature contains several recent studies on the effect of pressure on the phase separation temperature of binary polymer mixtures exhibiting both upper and lower critical solution temperatures. Walsh initiated an early series of studies on polymer-polymer demixing behavior.[12-14] In blends of chlorinated polyethylene and a poly(ethylene vinyl acetate) copolymer, optical cloud point measurements revealed a shift of the LCST of +14 °C at 750 atm (~20 °C/kbar). Also reported were measurements of poly(ether sulfone) and poly(ethylene oxide) blends, which showed a shift of the LCST of +16 °C at 348 atm (~46 °C/kbar).[12] Based on an estimate of the heat of mixing obtained using low molecular weight analogs, negative volumes of mixing values were predicted, of order 1×10^{-4}.[12]

Schwahn, et al. also studied the effect of pressure on phase equilibria in both UCST and LCST systems. Blends of deuterated poly(styrene) and poly(phenyl methyl siloxane) showed an accessible UCST, and LCST phase behavior was studied using blends of deuterated poly(styrene) and poly(vinyl methyl ether). The spinodal temperature, T_s, was determined using pressure-dependent SANS by extrapolating the inverse scattering intensity to zero wavevector. In both cases, T_s increased with pressure. In the former system, the pressure coefficient of the UCST was +12 °C/kbar, and for the latter LCST system, the coefficient was +43 °C/kbar.[6-9]

Meier examined the pressure dependence of the UCST in poly(ethylmethylsiloxane)/poly(dimethylsiloxane) blends. A SANS study showed that the transition temperature in this system decreased with pressure. The demixing curve had an initial slope of approximately -30 °C/kbar, while at pressures above 1 kbar the curve levelled out to value of -5 °C/kbar.[10] This was regarded as an unusual case of pressure-induced miscibilization in a blend with UCST phase behavior.

Frielinghaus, Schwahn, et al. have studied several blend and diblock copolymer systems using pressure-dependent SANS.[15-] In a separate study, the UCST in blends of deuterated poly(butadiene) and poly(styrene) increased with pressure by approximately 10 °C/kbar, while mixtures of poly(ethylethylene) and poly(dimethylsiloxane) first showed a reduction of the transition temperature, followed by a slight increase at higher pressures. Mixtures of deuterated poly(styrene) and poly(vinyl methyl ether) showed a linear increase of the LCST of approximately 15 °C/kbar.[16]

Hammouda and Bauer reported pressure enhanced miscibility in both deterated poly(styrene)/poly(vinyl methyl ether) blends and in deuterated poly(styrene)/poly(butyl methacrylate) blends. These blends show LCST behavior. However, the positive pressure coefficient was not quantified in this study.[17]

C. Discussion

Block Copolymer Trends. Although there have been few careful studies of the UODT phase transition reported in the literature, the available data display a wide range of transition temperatures and chain lengths. In Figure 4.2, the transition

temperatures, T_{trs}, for several UODT systems are plotted versus the average number of monomers in the chain, N_{avg}, assuming two backbone methylene carbons represent one monomer. Included in this figure are data from three lamellar diblock copolymers: poly(styrene-*block*-isoprene) (PS-PI)[1], poly(styrene-*block*-n-vinyl pyridine) (PS-PVP)[2], and poly(ethylene-*block*-ethylene-co-propylene) (PE-PEP)[3]; the LDOT poly(*d*-styrene-*block*-n-butyl mechacrylate) (dPS-PBMA) is also shown for comparison.

A number of trends are clearly evident when they are shown in this form. First, all systems show a transition temperature which is linear with chain length, within the experimental error and the limited range of transition temperatures covered by the experiments. This can be rationalized by a simple scaling argument. At the phase transition, the critical interaction parameter, χ_{trs}, is inversely proportional to the molecular weight, $\chi_{trs} \sim 1/N$.[22] Combining this with the Flory-Huggins form for the interaction parameter, $\chi \sim 1/T$, implies that the transition temperature will rise linearly with the molecular weight, $T_{trs} \sim N$, as shown in the figure. Second, there is a factor of ten difference in the critical chain length displayed by the PE-PEP, compared to the well-studied model system, PS-PI. This observation can also be justified through Liebler's parametrization of the critical condition required for phase separation, $(N\chi)_{trs} \sim 10$, which captures the inverse relation between the system energy (expressed through χ) and the system entropy (which scales with the chain length, N). Since the interactions between the PE block and the PEP block are weak (as intuitively expected in olefinic systems), and χ is therefore low, much higher degrees of polymerization can be tolerated before the critical condition is met and the ordered state becomes the equilibrium phase.

Finally, the transition lines shown in Figure 4.2 have high slopes, indicating that the phase separation temperature is very sensitive to small changes in the molecular weight. A best-fit line through the data points is included in the figure shows that, as the interactions progressively weaken across the figiure, the slope appears to change in proportion:

PS-PVP: 1.5 °C/monomer (N_c~200)

PS-PI: 0.5 °C/monomer (N_c~400)

PE-PEP: 0.03 °C/monomer (N_c~1500)

This trend can be rationalized by examining the coefficient of proportionality from the scaling argument given above. The Flory-Huggins interaction parameter is defined to be proportional to the monomeric exchange energy, $\chi \sim \Delta\varepsilon/T$, where $\Delta\varepsilon = \varepsilon_{12} - (\varepsilon_{11} + \varepsilon_{22})/2$. This implies $T_{trs} \sim \Delta\varepsilon/\chi_{trs}$. Since $\chi_{trs} \sim 1/N$, we therefore expect $T_{trs} \sim (\Delta\varepsilon)N$. The proportionality constant in this equation shows the slope will be higher in more strongly interacting systems, a trend that is is observed in the systems here.

p(*d*-S-*b*-nBMA) Trends. As shown in Figure 4.2, the transition temperature of p(*d*-S-*b*-nBMA), established in Chapter II, drops rapidly with an increase of molecular weight. Using the conventional description of the critical conditions required for phase separation, $(N\chi)_{trs} \sim 10$, we conclude that χ increase with temperature, where χ now represents all noncombinatorial contributions to the free energy. Although a variety of functional forms have been proposed for χ in cases when the bare Flory-Huggins term (~1/T) is overtaken by additional terms, we assume here that a simple linear form, $\chi \sim T$, is dominant. If $\chi \sim T$, then we expect $T_{LDOT} \sim N^{-1}$. This inverse dependence of molecular weight stands in direct contrast to the linear dependence shown by the UODT systems. A best-fit of the limited data to this functional form is

shown in Figure 4.3, and yields T_{LDOT} (K) = 100 + 23000 N_{avg}^{-1}, for $\phi_{dPS} \sim 0.5$. This equation can be conveniently employed for interpolation, and it may be of use in guiding the synthesis of new block copolymers where there is a desire to control the transition temperature. However, it is important to note that, due to the insufficient range of data available and high level experimental error in determining the molecular weight and component volume fractions, these data can not be used as *proof* that the transition temperature scales with N^{-1}. The two forms $T_{LDOT} \sim N^{-1}$ and $T_{LDOT} \sim N$ (which is suggested by Figure 4.2) are in fact indistinguishable using these data, based on the correlation coefficients obtained from linear, least-squares fits. Therefore, we suggest the following interpretation: if the Leibler criterion is an accurate description of the critical condition required for phase separation when there are additional, noncombinatorial contributions to the free energy, as expected in the case of p(*d*-S-*b*-nBMA), then we expect the transition temperature to be inversely proportional to N.

Examining the interaction parameter of the parent homopolymers reveals some trends in the phase behavior of the constitutent diblocks. Balsara summarized the relevant work on ambient-pressure phase behavior in binary polymer blends in terms of the simple Flory-Huggins analysis.[5] In his review, an empirical expression of the type $\chi \sim A + B/T + C/T^2$ is employed so that a wide variety of phase diagrams can be incorporated into the traditional framework. The LCST is accomodated by allowing B to have negative values; the additional C/T^2 term allows for curvature in the 1/T plane and, therefore, simultaneous LCST/UCST or closed-loop phase behavior. The constant A is usually denoted the entropy term, which is typically used to combine all the noncombinatorial entropy contributions that are neglected in the original Flory-

Huggins treatment. The constant B is usually called the energy term, and it reflects the temperature sensitivity of the interactions (as implied by $\chi \sim \Delta\varepsilon/T$). The trend from all the literature data summarized by Balsara is that all blends with LCST type phase behavior have large and negative energy terms, and moderately high and positive entropy terms. These data are summarized in Figure 4.4, where the values of the entropy term are plotted versus the energy term for all the LCST systems reported. This is a rather suggestive form to display these empirical terms, since it reveals a trend between the two parameters, both tend to increase simultaneously when PS is the first component. This characteristic is not observed in the (more numerous) UCST systems.

As shown in Figure 4.4, the parent homopolymers of interest, dPS and PBMA are miscible and are characterized by an interaction parameter of the form, $\chi(T) = 0.10 - 60/T$, indicating both the strong temperature sensitivity and large noncombinatorial contributions to the total entropy in this LCST system. An estimate of $\chi(T)$ in p(*d*-S-*b*-nBMA) can be obtained from the SANS data in Chapter 2. The disordered-state scattering function of block copolymers has the form $I(Q) \sim N\,[F(Q)-2\chi N]^{-1}$. With absolute intensity calibration, and knowledge of chain parameters, χ is an unknown parameter that can be determined through fitting the 1-dimensional SANS profiles to this scattering function. Since the temperature resolution of the SANS experiment was extermely low, and therefore too few data points taken in the disordered state at ambient pressure, we fit the scattering function instead to profiles obtained at high pressure, where there 7 temperature increments. There, the 85k p(*d*-S-*b*-nBMA) is in the disordered state, with a projected LDOT above 250 °C. Under these conditions, we obtain $\chi(T) = 0.037 - 10.5/T$. As discussed in the molecular weight dependence above,

the experimental resolution of these experiments is not sufficient to prove the 1/T form of the interaction parameter in this system, and in fact the temperature dependence obtained from these scattering measurements may also be described by a ~T form, to an extremely high degree of precision. We employ the ~1/T form because its usage is established, regardless of interpretation.

This result compares favorably with estimates obtained by Ruzette, et al who have also studied these LDOT systems extensively. In considering the unusual phase behavior of these diblock copolymers, they approached the problem by synthesizing a variety of diblock copolymers, varying only the size of the pendant alkyl group $(CH_2)_n$ in the methacrylate block. This structure-property approach led to the observation that for $n < 3$, e.g. methyl- and ethyl- methacrylates, UODT phase behavior was observed, while the moderately-sized groups led to LDOT phase behavior. Increasing n further led to a return of the UDOT. These observations were made by observing the trends in the SANS profiles, since in many cases the transition itself was thermally inaccessible. This window in the phase behavior where the LDOT is observed in sytrene-methacrylate systems corresponds closely to the difference in solubility parameters of the parent hompolymers. The resulting solubility parameter argument led to the following conclusion: if the parent homopolymers have sufficiently similar cohesive energy densities, then a diblock copolymer formed from those constitutent monomers might show miscibility for some limited range of molecular weights, and therefore have potential to show an accessible LDOT. If instead the parent homopolymers have even moderate differences in their cohesive energy densities, then the diblock copolymer will always show UODT phase behavior, and therefore prevent any appearance an LDOT. This work appears to suggest that successfully engineering the

LDOT into unknown chemical systems rests mostly on matching the repulsive interactions between A and B monomers to eliminate any encroachmant of the UDOT.

In that study, the styrene-methacrylate systems with conventional UODT phase behavior had interactions parameters with moderate temperature dependences and high entropic constants. For n = 12, poly(styrene-*block*-lauryl methacrylate), they obtained $\chi(T) = 0.063 + 9.32/T$, for n = 8, poly(styrene-*block*-octyl methacrylate), they obtained $\chi(T) = 0.039 + 7.57/T$, and for n = 6, poly(styrene-*block*-hexyl methacrylate), they obtained $\chi(T) = 0.035 + 3.93/T$. These are UODT systems. However, due apparently to the lack of a theoretically justifiable form for $\chi(T)$ that permits an LDOT, they did not publish any values of the interaction parameter for n = 3 or n = 2 which showed LDOTs. Our result for comparison is $\chi(T) = 0.037 - 10.5/T$. The trend therefore appears to be that shortening the length of the pendant group in the UODT systems results in a diminishing value of both the entropic constant and the energetic term, a trend towards athermal mixing. We note that only the trends are important in these studies since a variety of functional forms could be used to describe $\chi(T)$, and in fact the presence of a scaling factor in the fitting procedure is not strictly justifiable on theoretical grounds. Further comments on the nature of the interactions in these systems should not be pursued within the context of Flory-Huggins theory, and it is hoped that new theoretical developments which directly assess volume and packing effects will allow a more suitable description of these trends.

Transition Analysis. In a one-component system, two rules apply to the phase transition line in a P-T diagram: (i) the higher pressure phase always has the greater density; and (ii) the higher temperature phase always has the higher molar entropy. Alternatively stated, in a P-T phase diagram, the phase lying in the direction of

increasing P as the phase transition line is crossed (i.e., isothermally) has the greater density, and the phase lying in the direction of increasing T as the phase transition line is crossed (i.e., isobarically) has the greater entropy. These simple arguments follow from the definition of the Gibbs free energy function and its derivatives (which are measurable material properties) for a one-component system.

These rules are consistent with the Clapeyron equation, which relates the slope of the phase transition line in the P-T plane to the entropy and volume changes suffered by the material as the phase transition is traversed. The Clapeyron equation is derived by equating the chemical potentials between two coexisting phases suffering an infinitesimal displacement. For the independent variables p and T, the equation is expressed in the following form: $dp/dT = (S_2 - S_1)/(V_2 - V_1)$ where the numerator is the difference in molar entropy between the two phases, and the denominator is the difference in molar volume between the two phases, at the transition. The Clapeyron equation has been used successfully in numerous instances to correlate phase behavior in a variety of one-component phase equilibria, since knowledge of two of the unknowns in this equation allows prediction or estimation of the third. A relevant example is the study of thermotropic liquid crystals, materials which display a wide variety of phase complexity in both the temperature and pressure variables.[3]

There are several consequences of this analysis relevent to the phase behavior of block copolymers. First, it requires that the transition from disorder to order at a UODT proceed exothermically. The UODT is usually understood as an enthalpy-driven transition, since by locally phase separating as the material is cooled, the monomeric segments increase the number of favorable A-A and B-B contacts, and lower the number of repulsive A-B contacts. The latent heat required to melt this

structure, i.e. through heating, produces an endotherm which should be osbservable through calorimetry measurements. Mean-field theory with a characteristic exchange energy describes this type of behavior. By contrast, the transition from disorder to order at an LDOT must proceed endothermically, or accompanied by an entropy gain, since it is accessed by increasing the temperature. Melting this structure, by cooling, will therefore produce an exotherm. This prediction is counterintuitive, since block copolymer ordering is accompanied by a *loss* of translational and positional entropy, due to the restriction of the chain's junction point in the interfacial region. In order to expect an entropy *gain* when the chains locally segregate, there must be some kind of entropic restriction in the disordered state that becomes relaxed when the ordered state is formed. Although we speculate that this negative entropy contribution could arise from the lack of free volume of the mixed state relative to the hypothetical unmixed state of the two parent homompolymers, firm conclusions about the origin and nature of these effects are rarely encountered in the literature. To highlight these effects, the LCST and LDOT phase behaviors are commonly discussed as entropy driven transitions.

In the case of diminishing ΔS_{ord} and ΔV_{ord}, the ratio in the Clapeyron equation is indeterminate. An alternative formulation of the Clapeyron equation can be obtained by substituting differentials for the integral enthalpy and volume changes. The following two equations are obtained:

$$(1) \qquad dp/dT = (C_{p,2} - C_{p,1})/[V_{mol}T(\alpha_2 - \alpha_1) = \Delta C_p/V_{mol}T\Delta\alpha$$

$$(2) \qquad dp/dT = (\alpha_2 - \alpha_1)/(K_2 - K_1) = \Delta\alpha/\Delta K$$

where C_p is the constant-pressure heat capacity, α is the thermal expansion coefficient, and K is the isothermal compressibility. These equations can be used in correlating

phase behavior for continuous transitions, since the first order quantities for these transitions are zero.

For a block copolymer with a UODT and a positive pressure coefficient, Eq. 2 shows that if the thermal expansion of the disordered state is greater than that of the ordered state, then the disordered state must also have a larger compressibility. This is intuitively reasonable, since a melt with a greater expansivity has more free volume which is readily expendable by the application of pressure. By contrast, the positive pressure coefficient observed in the case of the LDOT requires now that the ordered state have the greater expansivity and compressibility. This is supported by the expectation of a positive change in specific volume upon ordering, which gives the ordered state a larger free volume. Alternatively stated, the disordered state in this case must lack free volume relative to the ordered state. A possible reason for this behavior, often cited in the literature discussions, is unequal packing between the monomers. The exchange of A–A and B–B contacts for A–B contacts occurs in an nonideal fashion, resulting typically in a total volume reduction and the loss of free volume. Due to the intricate and subtle nature of van der Waals interactions and monomer packing, very few studies have been undertaken to correlate mixing effects and phase behavior based on the shape and size of the constituent monomers.

Effect of deuteration. One advantage of neutron scattering is that deuterium labelling provides atomic scattering contrast with only minimal disruption of the total interaction energy. However, the small change in the zero-point energy of the C-D bond, summed over many atoms, can exert profound effects on the observable phase behavior.[23] In PS/PVME blends, deuterating the pendant benzene ring of the PS has

been shown to shift the LCST by ~40 °C.[24] Since deuteration of the PS chain backbone had little effect on the demixing temperature, this was interpreted as evidence that the misicibility in this system is controlled to some extent by interactions involving the benzene ring.

A similar effect is observed in p(*d*-S-*b*-nBMA) diblock copolymers. The effect of deuteration of the benzene ring component in these diblock copolymers shifts the LDOT by ~50 °C. This is illustrated in Figure 4.5, which shows the LDOTs of p(*d*-S-*b*-nBMA) as a function of molecular weight. These values were determined by SANS or static birefringence measurements. They are shown alongside the LDOT of the nondeuterated counterpart, p(*d*-S-*b*-nBMA) of similar molecular weight, which was recently observed.[25] This observation suggests that, as in the PS/PVME blend system, subtle interactions involving the benzene ring play an important role in the compatibility observed in this system. This is particular noteworthy in view of Figure 4.4, which shows that PS forms a number of miscible blends with chains containing the carbonyl or ether groups.

D. References

[1]Liquids and liquid mixtures. Rowlinson, J. Plenum Press, 1969.

[2]Thermodynamics, an advanced treatise for chemists. Guggenheim, E. Amsterdam Publ. Co., 1967.

[3]Phase Transitions in Liquid Crystals. NATO ASI Series, Martellucci, S.; Chester, A., Eds. Plenum Press, 1992.

[4]Handbook of Liquid Crystals, Vol. I. Demus, D.; Goodby, G.; Gray, G.; Spiess, H.-W.; Vill, V. Wiley-VCH, 1998.

[5]Russell, T. P.; Karis, T. E.; Gallot, Y.; Mayes, A. M. *Nature* **1994**, *368*, 729.

[6]Pressure dependence of the Flory-Huggins interaction parameter in polymer blends: A SANS study and a comparison to the Flory-Orwell-Vrij equation of state. Janssen, S.; Schwahn, D.; Mortensen, K.; Springer, T. *Macro.*, **1993**, *26*, 5587.

[7]Coil and melt compressibility of polymer blends studied by SANS and pVT experiments. Janssen, S.; Schwahn, D.; Springer, T.; Mortensen, K. *Macro.*, **1995**, *28*, 2555.

[8]Investigation of the pressure dependence of the Gibbs potential for polymer blends by means of SANS. Janssen, S.; Schwahn, D.; Springer, T.; Mortensen, K.; Hasegawa. *Physica B*, **1995**, *213-214*, 691.

[9]Pressure Dependence of the order-to-disorder transition in polystyrene/polyisoprene and polystyrene/ poly(methylphenylsiloxane) diblock copolymers. Steinhoff, B.; Rüllmann, M.; Wenzel, M.; Junker, M.; Alig, I.; Oser, R. Stühn, B.; Meier, G.; Diat, O.; Bösecke, P.; Stanley, H. *Macro.* **1998**, *31*, 36.

[10]Pressure Dependence of the order-to-disorder transition in polystyrene/polyisoprene and polystyrene/ poly(methylphenylsiloxane) diblock copolymers. Steinhoff, B.; Rüllmann, M.; Wenzel, M.; Junker, M.; Alig, I.; Oser, R. Stühn, B.; Meier, G.; Diat, O.; Bösecke, P.; Stanley, H. *Macro.* **1998**, *31*, 36.

[11]Pressure-induced compatibility in a model polymer blend. Beiner, M.; Fytas, G.; Meier, G.; Kumar, S. *Phys. Rev. Lett.* **1998**, *81*, 594.

[12]Effect of pressure on polymer-polymer phase separation behavior. Walsh, D.; Rostami, S. *Macro.*, **1985**, *18*, 216.

[13]Simulation of upper and lower critical phase diagrams for polymer mixtures at various pressure. Rostami, S.; Walsh, D. *Macro.*, **1985**, *18*, 1228.

[14]Pressure-volume-temperature properties and equations of state in polymer blends: characteristic parameters in polystyrene/poly(vinyl methyl ether) mixures. Ougizawa, T.; Dee, G.; Walsh, D. *Macro.*, **1991**, *24*, 3834.

[15]Temperature- and pressure-dependent composition fluctuations in a polybutadiene/polystyrene polymer blend and diblock copolymer. Frielinghaus, H.; Abbas, B.; Schwahn, D.; Willner, L. *Europhys. Lett.*, **1998**, *44*, 607.

[16]Pressure and temperature effects in homopolymer blends and diblock copolymers. Frielinghaus, H.; Schwahn, D.; Mortensen, K.; Willner, L.; Almdal, K. *J. Appl. Cryst.*, **1997**, *30*, 696.

[17]Small-angle neutron scattering from deuterated polystyrene/poly(butyl methacrylate) homopolymer blend mixtures. Hammouda, B.,; Bauer, B.; Russell, T. *Macro.*, **1994**, *27*, 2357.

[18]High-pressure effects on the order-disorder transition in block copolymer melts. Hajduk, D.; Gruner, S.; Erramilli, S.; Register, R.; Fetters, L. *Macro.* **1996**, 1473.

[19]Change of phase behavior of diblock copolymers upon application of pressure. Bartels, V.; Stamm, M.; Mortensen, K. *Polym. Bull.* **1996**, *36*, 103.

[20]Temperature and pressure dependence of the order parameter fluctuations, conformational compressibility, and the phase diagram of the PEP-PDMS diblock copolymer. Schwahn, D.; Frielinghaus, H.; Mortensen, K.; Almdal, K. *Phys. Rev. Lett.* **1996**, *77*, 3153.

[21]Small angle neutron scattering studies on phase behavior of block copolymers. Hasegawa, H.; Sakamoto, N.; Takeno, H.; Jinnai, H.; Hashimoto, T.; Schwahn, D.; Frielinghaus, H.; Janssen, S.; Imai, M.; Mortensen, K. *J. Phys. Chem. Solids*, **1999**, *60*, 1307.

[22]Theory of microphase separation in block copolymers. Leibler, L. *Macro.* **1980**, *13*, 1602.

[23]Thermodynamics of isotopic polymer mixtures: poly(vinyl ethylene) and poly(ethyl ethylene). Bates, F.; Fetters, L; Wignall, G. *Macro.*, **1988**, *21*, 1086.

[24]Phase diagrams of poly(vinylmethylether)-selectively deuterated polystyrene: an original route to the precise nature of polymer-polymer interactions. Larbi, F.; Leloup, S.; Halary, J.; Monnerie, L. *Polym. Comm.*, **1986**, *27*, 23.

[25]Vogt, B., U. of Massachusetts, personal communication.

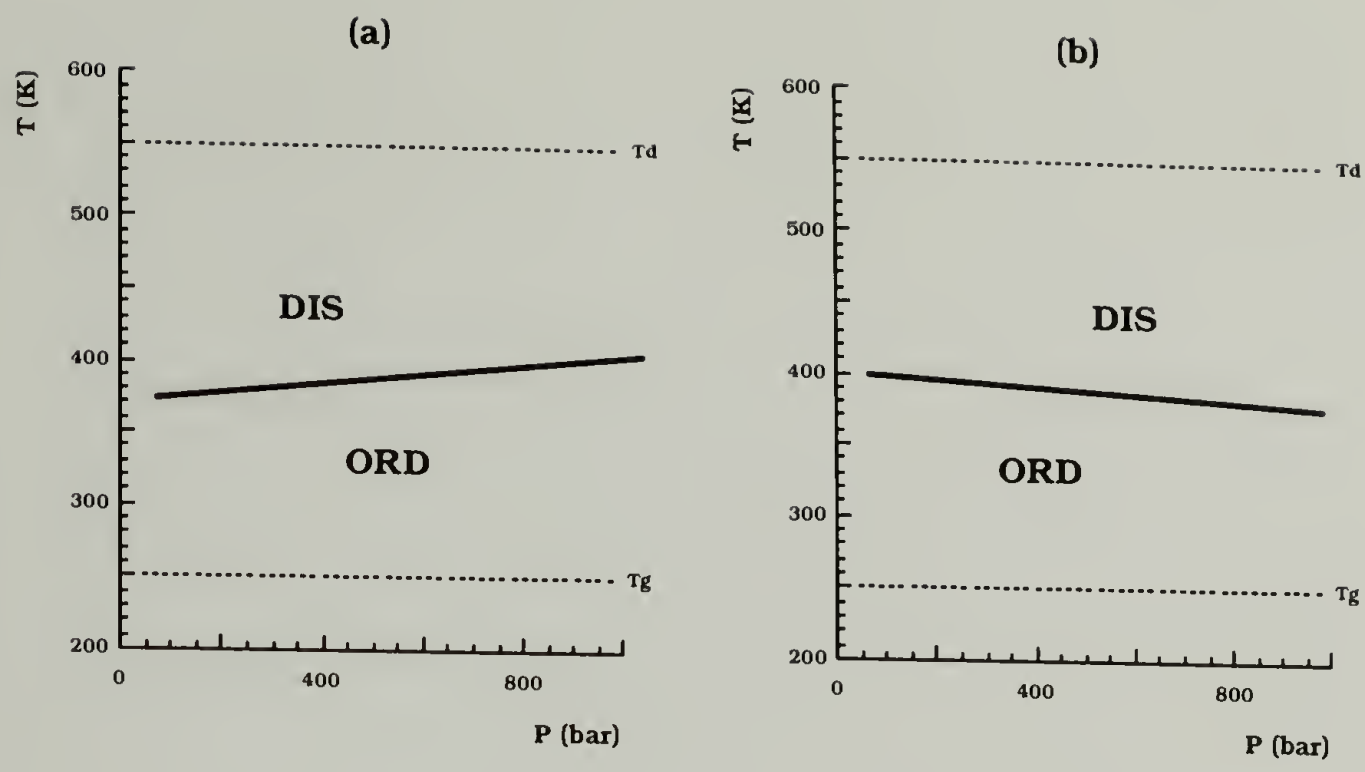

Figure 4.1 Schematic block copolymer phase diagrams. Diagrams (a) and (b) show typical positive and negative pressure coefficients for one-component UODT systems, and (c) shows the unusual case of curvature of the phase transition line. The results obtained in the LDOT system, p(*d*-S-*b*-nBMA), are shown in (d).

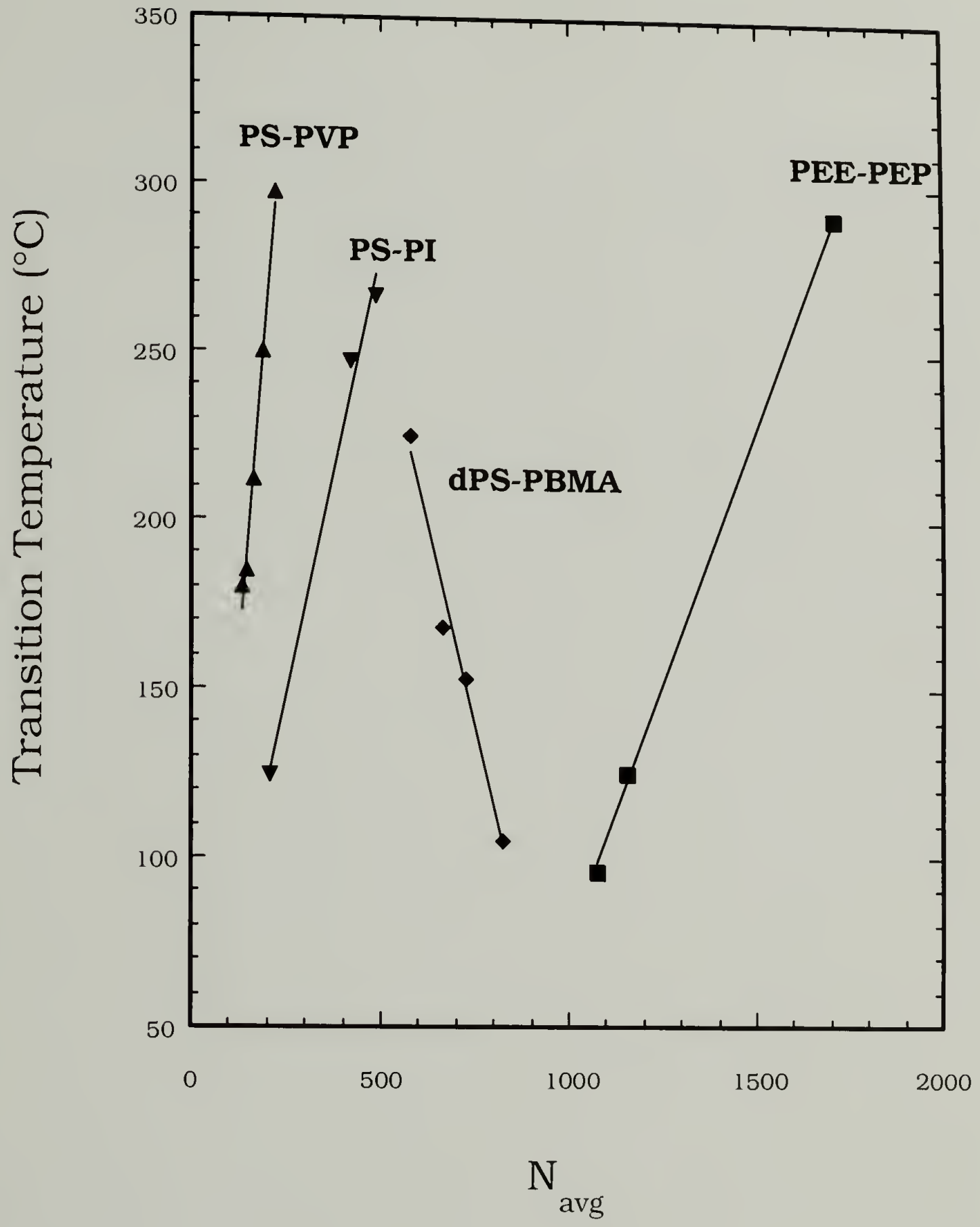

Figure 4.2 Transition temperatures, UODT and LDOT. Summary of transition temperatures reported in the literature for block copolymers with $N_A = N_B$. UODTs: PS-PVP (Schulz), PS-PI (Khandpur), PE-PEP (Bates). LDOTs: PS-PBMA.

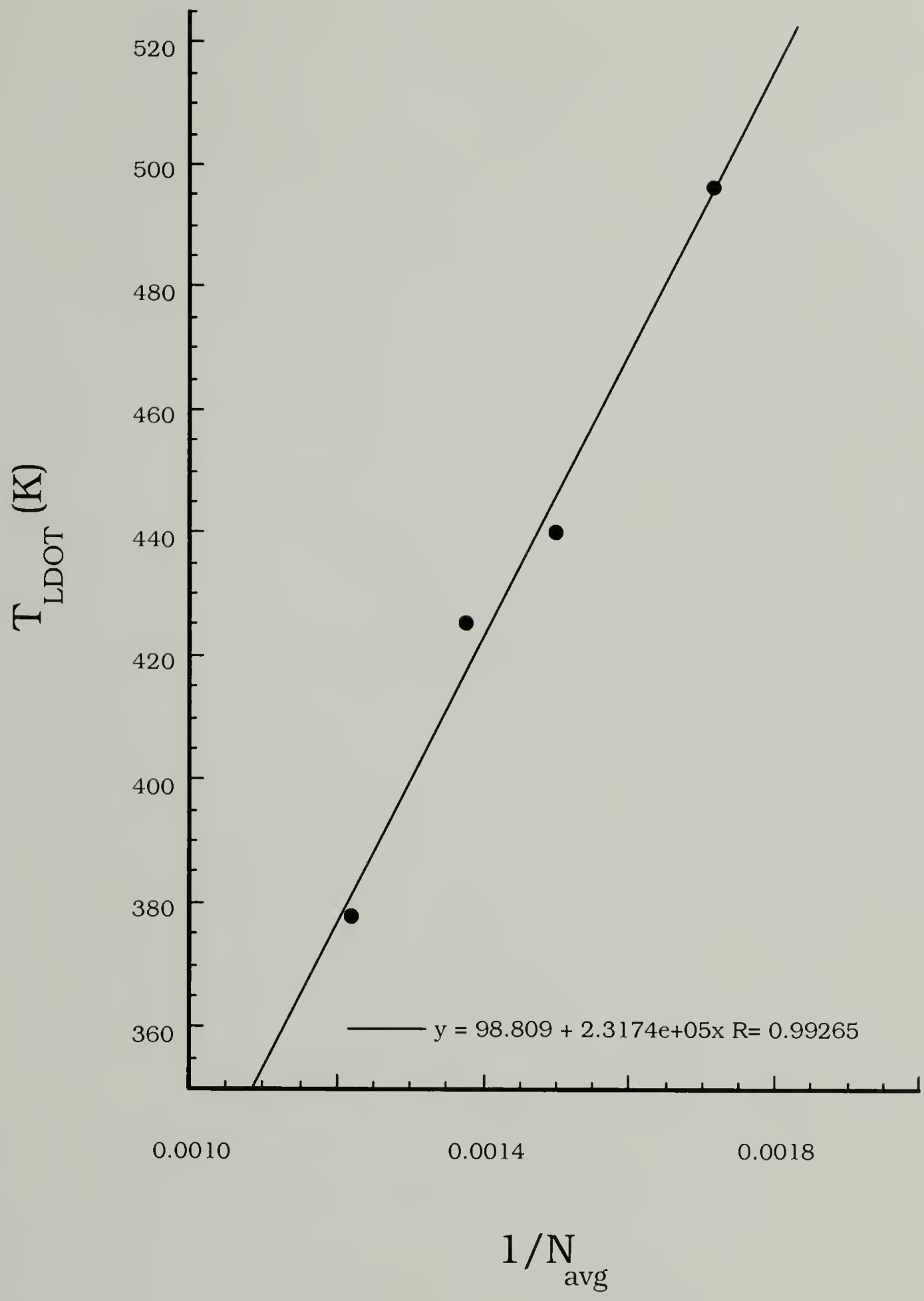

Figure 4.3 Best fit of transition temperatures. The fit yields the approximate expression T (K) = 100 + 23 000 N^{-1} for p(*d*-S-*b*-nBMA).

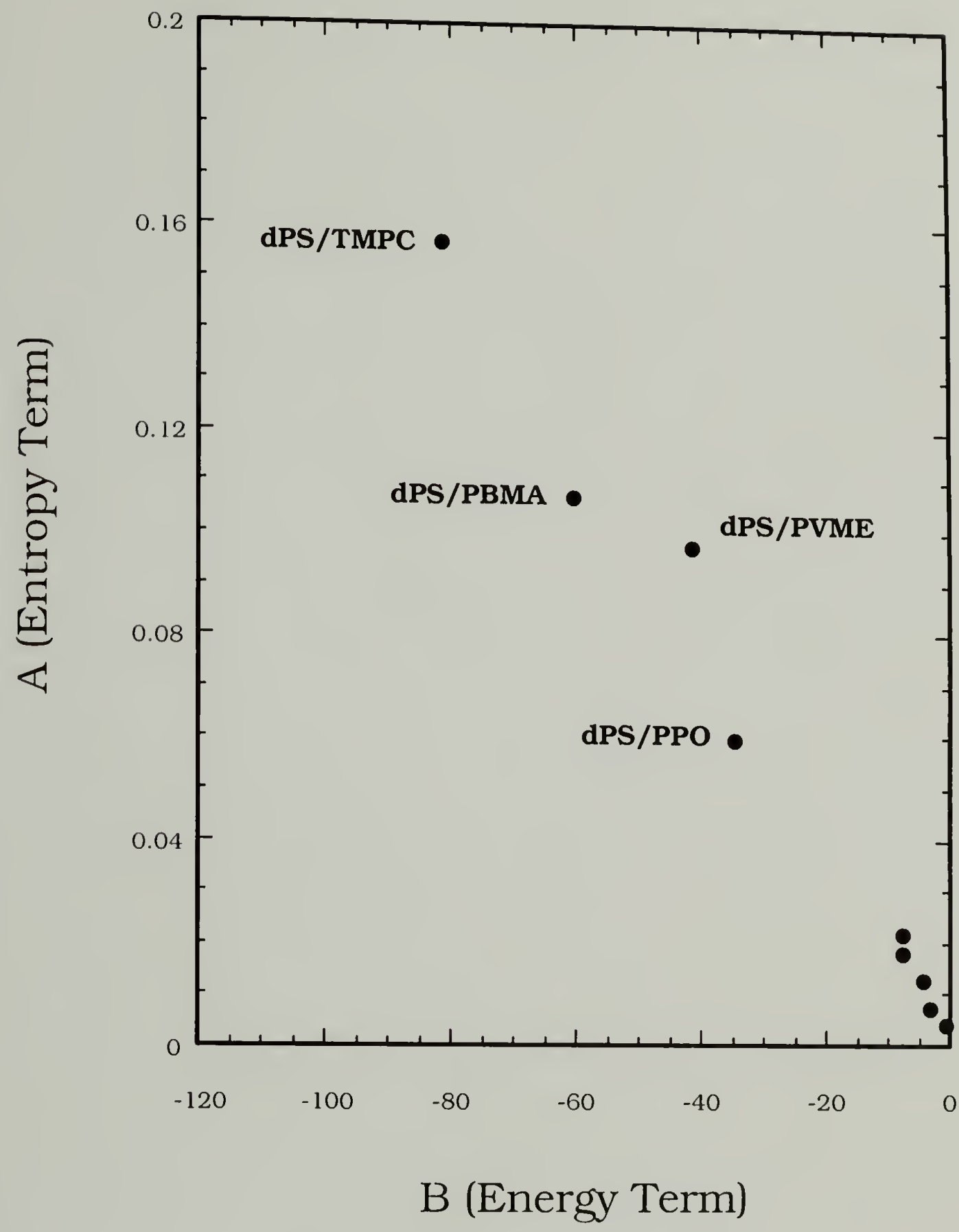

Figure 4.4 Flory-Huggins parameters in LCST blends. Literature compilation for miscible blend pairs, where $\chi \sim A + B/T$. TMPC refers to tetramethyl-bisphenol A polycarbonate, PPO to dimethyl phenylene oxide, PVME to poly(vinyl methyl ether), and PBMA to poly(n-butyl methacrylate). Unmarked points refer to olefinic systems.

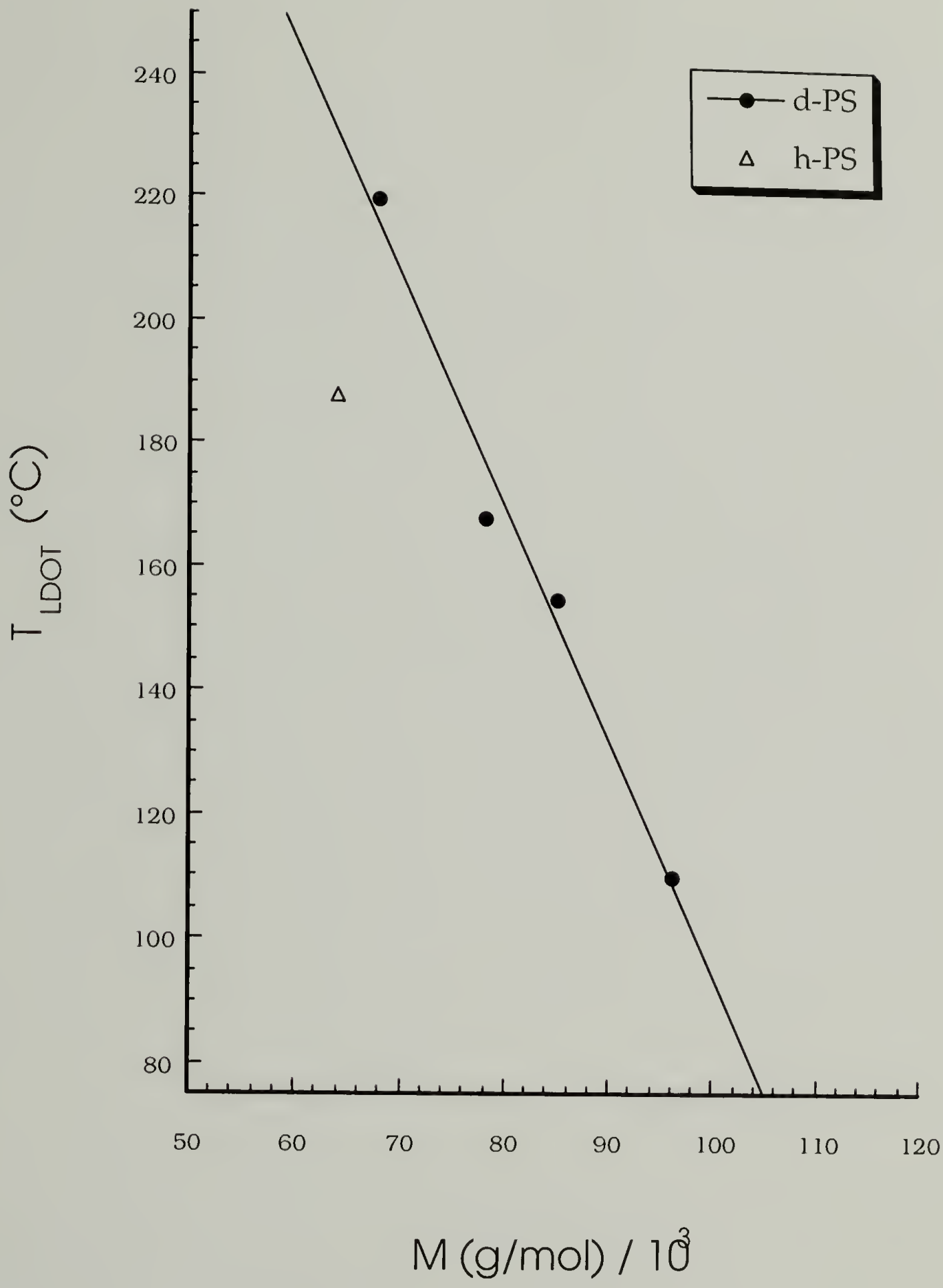

Figure 4.5 Deuteration effect in p(S-*b*-nBMA). with $N_A = N_B$ (lamellar morphology). p(S-*b*-nBMA)[25] and p(*d*-S-*b*-nBMA) values taken from static birefringence measurements or SANS data. A regression line is shown as a guide for the eye.

CHAPTER 5

CONCLUSIONS

The studies described here were undertaken to extend and explore the phase behavior of a diblock copolymer system showing the thermally accessible microphase separation transition upon heating. This was denoted the LDOT, or lower disorder to order transition, in analogy to the LCST observed in partially miscible blends which demix upon heating. Analogous LCST type phase diagrams observed in polymer blends are potentially more interesting than the typical UCST type because excess mixing volume and enthalpy, equation-of-state effects, make dominating contributions. A general rule is that the phase separation temperature is much more sensitive to the application of pressure than in typical UCST systems. This provided the initial motivation to investigate the pressure-dependence of the LDOT in p(*d*-S-*b*-nBMA)

The pressure coefficient of this phase transition was determined using in-situ high pressure SANS. The value of ~150 °C/kbar, established for p(*d*-S-*b*-nBMA) with equivalent block lengths, is greater by a factor of ~7 than the previously published results for UODT diblock copolymers. The pressure sensitivity inherent in the global demixing behavior of miscible blends with an LCST is, therefore, also observed in the case of local demixing of phase-mixed diblock copolymers with an accessible LDOT. This is the central message of this thesis. In order to make contact with the recent data obtained for block copolymers with conventional UODT phase behavior, studies were then begun to measure the transition volume change, ΔV_{ord}, and enthalpy change, ΔH_{ord}, both expected to be positive, for p(*d*-S-*b*-nBMA). Both quantities proved

exceedingly difficult to measure for this system, due probably to a combination of the weak first-order nature of this transition, poorly understood kinetic factors, and lack of operator expertise in the demanding techniques required for measurement.

Several encouraging observations were made in these experiments, however, which require further study. (1) The reduction in free volume accompanying mixing is usually attributed to equation-of-state effects in the literature, yet these are rarely quantified. The use of x-ray reflectivity to measure thin film thermal expansion is a precise method that may yield an accurate measure of these excess volume effects. The observation of significantly decreased expansion coefficients in p(d-S-b-nBMA) in the disordered state, can be used to quantify this effect since the excess mixing volume (negative in this case) is directly related to thermal expansion. The construction, for example, of the $\alpha(\phi)$ curve, where ϕ is the volume fraction of the blend of the two parent homopolymers, may result in useful equation of state information applicable to the blend case, which may then be used as a guide in interpreting the behavior from the respective diblock copolymers.

(2) A second avenue of further investigation concerns the kinetics of ordering from the quiescent melt state. For such rough measurements, the optical microscope observations discussed in Chapter 3 show surprising linearity between the onset time of ordering and the quench temperature, over the widest range of temperatures resolvable. This simple correlation appears unusual given the complexity of ordering, where the onset time reflects a competition between the nucleation of ordered domains and their growth to observable dimensions, and only indirectly reflects local microphase separation. It has been shown that ordering is often hindered or modified by the presence of the glass transition of one or both blocks; some simplification may

result from the viscous conditions prevailing at these ordering temperatures. An interesting dimension to this problem is the role reversal of temperature in establishing the quench depth and the requirement that ordering be endothermic. Careful experiments should be pursued to clarify further this ordering process and interpret the observed linear behavior.

(3) It is interesting to note the recent study of Frielinghaus, who performed high pressure experiments in diblock copolymers and blends of their parent homopolymers. This appears to be the first study directly comparing blends and diblock copolymers having the same components. This kind of study is motivated by the need to understand how the covalent junction point tying A and B together alters the phase behavior. In this case, the pressure dependence of the UCST or UODT was studied. Blends of deuterated poly(styrene) and poly(butadiene) first showed a linear increase of the UCST. Surprisingly, the UODT of poly(styrene-*block*-butadiene), was observed to remain constant up to 200 MPa.[15] The expected behavior is for the mixture trends to be reproduced in the diblock copolymer, but no rationale was offered for this unusual occurrence. A reasonable suggestion is that there are large volume and enthalpy contributions associated with the mixing in the interfacial region between the A and B domains which is not present in the phase-separated blend. The relative contribution of these two quantities will depend on the nature of the interactions and complex monomeric packing effects, and therefore on the specific chemical system. Similar reasoning should apply in the case of LCST systems. However, there are no quantitative pressure data on the dPS/PBMA blend system, though qualitative results were reported by Hammouda. No contrast with the p(*d*-S-*b*-nBMA) results can be offered. Further work in this area should be devoted to a quantitative determination of

the pressure coefficient of the demixing temperature in these blends, in order to draw a contrast with the sensitive pressure dependence observed in the case of diblock copolymers composed of these polymers.

BIBLIOGRAPHY

Studies Relevant to p(S-*b*-nBMA)

Russell, T. P.; Karis, T. E.; Gallot, Y.; Mayes, A. M. *Nature* **1994**, *368*, 729.

Rheology of the lower critical ordering transition. Karis, T. E.; Russell, T. P.; Gallot, Y.; Mayes, A. M. *Macro.* **1995**, *28*, 1129.

The effect of hydrostatic pressure on the lower critical ordering transition in diblock copolymers. Pollard, M.; Russell, T.; Ruzette, A.; Mayes, A.; Gallot, Y. *Macro.* **1998**, 6493.

Phase behavior of diblock copolymers between styrene and n-alkyl methacrylates. Ruzette, A.-V. G.; Banerjee, P.; Mayes, A. M.; Pollard, M.; Russell, T. P.; Jerome, R.; Slawecki, T.; Hjelm, R.; Thiyagarajan, P. *Macro.* **1998**, *24*, 8509.

Phase Transitions in Polymer Blends and Block Copolymers induced by Selective Dilation with Supercritical CO_2. Watkins, J. J.; Brown, G. D.; Pollard, M. A.; Ramachandrarao, V. S.; Russell, T. P. *Supercrit. Fluids* **2000**, 277.

Phase Separation in Polymer Blends and Diblock Copolymers Induced by Compressible Solvents. Watkins, J. J.; Brown, G. D.; RamachandraRao, V. S.; Pollard, M. A.; Russell, T. P. *Macro.* **1999** *32*, 7737.

Compressibility effects in a solvated polystyrene-polyisoprene diblock copolymer. Hammouda, B.; Lin, C.; Balsara, N. *Macro.* **1995**, *28*, 4765.

Small-angle neutron scattering from deuterated polystyrene/poly(butyl methacrylate) homopolymer blend mixtures. Hammouda, B.,; Bauer, B.; Russell, T. *Macro.* **1994**, *27*, 2357.

Synergism for the improvement of tensile strength in block copolymers of polystyrene and poly(n-butyl methacrylate). Weidisch, R.; Michler,G. H.; Arnold, M.; Hofmann, S.; Stamm, M.; Jérôme, R. *Macro.* **1997**, *30*, 8078.

Synthesis, dynamic-mechanical and morphological behavior of styrene/butyl methacrylate diblock copolymers. Arnold, M.; Hofmann, S.; Weidisch, R.; Michler, G.; Neubauer, A.; Poser, S. *Macromol. Chem. Phys.* **1998**, *199*, 31.

Schubert, D.; Weidisch, R.; Stamm, M.; Michler, G. *Macro.* **1998**.

Correlation between phase behavior and tensile properties of diblock copolymers.

Weidisch, R.; Stamm, M.; Schubert, D.; Arnold, M.; Budde, H.; Höring, S. *Macro.*, **1999**, *32*, 3405.

Weidisch, R.; Dissertation, Dr.-Ing., Universität Halle, 1997.

Narrow-polydispersity diblock and triblock copolymers of alkyl acrylates by a 'living' stable free radical polymerization. Listigovers, N.; Georges, M.; Odell, P,; Keoshkerian, B. *Macro.* **1996**, *29*, 8992.

Hashimoto, T.; Hasegawa, H.; Hashimoto, T.; Katayama, H.; Kamigaito, M.; Sawamoto, M.; Imai, M. *Macro.* **1997**, *30*, 6819.

Block Copolymers

Morphologies of block copolymers. Schulz, M.; Bates, F. *Physical Properties of Polymers*, Mark J., Ed., Ch 32, **1999**, 427.

Phase morphology in block copolymer systems. Thomas, E.; Lescanec, L. *Phil. Trans. R. Soc. Lond. A* **1994**, *348*, 149.

Theory of microphase separation in block copolymers. Leibler, L. *Macro.* **1980**, *13*, 1602.

Fluctuation effects in the theory of microphase separation in block copolymers. Fredrickson, G. H.; Helfand, E. *J. Chem. Phys.* **1987**, *87*, 697.

Density functional theory of lamellar ordering in diblock copolymers. Melenkevitz, J.; Muthukumar, M. *Macro.* **1991**, *24*, 4199.

Phase transition of an isotropic system to a nonuniform state. Brazovskii, S. *Sov. Phys. –JETP* **1975**, *41*, 85.

Polymer Blends

Thermodynamics of Polymer Blends. Balsara, N. *Physical Properties of Polymers*, Mark J., Ed., Ch. 19, **1999**, 257.

Polymer-polymer phase behavior. Bates, F. S. *Science* **1991**, *251*, 898.

Review. Bates, F. S.; Fredrickson, G. H. *Annu. Rev. Phys. Chem.* **1990**, *41*, 525.

Role of free volume changes in polymer solution thermodynamics. Patterson, D. *J. Polym. Sci., Polym. Lett.* **1968**, *16*, 3379.

Free volume and polymer solubility. A qualitative view. Patterson, D. *Macro.* **1969**, *2*, 672.

Thermodynamics of polymer compatibility. Patterson, D.; Robard, A. *Macro.* **1978**, *11*, 690.

Effects of molecular size and shape in solution thermodynamics. Patterson, D. *Pure & Appl. Chem.* **1976**, *47*, 305.

Aspects of polymer-polymer thermodynamics. McMaster, L. *Macro.* **1973**, *6*, 760.

Thermodynamics of isotopic polymer mixtures: significance of local structural symmetry. Bates, F.; Muthukumar, M.; Wignall, G.; Fetters, L. *J. Chem. Phys.* **1988**, *89*, 535.

Effect of molecular structure on the thermodynamics of block copolymer melts. Lin, C, Jonnalagadda, S.; Kesani, P.; Dai, H.; Balsara, N. *Macro.* **1994**, *27*, 7769.

Anomalous mixing behavior of polyisobutylene with other polyolefins. Krishnamoorti, R.; Graessley, W.; Fetters, L.; Garner, R.; Lohse, D. *Macro.* **1995**, *28*, 1252.

Regular and irregular mixing in blends of saturated hydrocarbons in polymers. Graessley, W.; Krishnamoorti, R.; Reichart, G.; Balsara, N.; Fetters, L.; Lohse, D. *Macro.* **1995**, 1260.

Chain-Packing effects in the thermodynamics of polymers. Londono, J.; Maranas, J.; Mondello, M.; Habenschuss, A.; Grest, G.; Debenedetti, P.; Graessley, W.; Kumar, S. *J. Polym. Sci., Polym. Phys.* **1998**, *36*, 3001.

Pressure - Polymer Blends.

High pressure thermodynamics of mixtures. Schneider, G. *Pure & Appl. Chem.*, **1976**, *47*, 277.

Effect of pressure on polymer-polymer phase separation behavior. Walsh, D.; Rostami, S. *Macro.* **1985**, *18*, 216.

Simulation of upper and lower critical phase diagrams for polymer mixtures at various pressure. Rostami, S.; Walsh, D. *Macro.* **1985**, *18*, 1228.

Pressure-volume-temperature properties and equations of state in polymer blends: characteristic parameters in polystyrene/poly(vinyl methyl ether) mixures. Ougizawa, T.; Dee, G.; Walsh, D. *Macro.* **1991**, *24*, 3834.

Pressure-induced compatibility in a model polymer blend. Beiner, M.; Fytas, G.; Meier, G.; Kumar, S. *Phys. Rev. Lett.* **1998**, *81*, 594.

Relationship between internal energy and volume change of mixing in pressurized polymer blends. Lefebvre, A.; Lee, J.; Balsara, N.; Hammouda, B.; Krishnamoorti, R.; Kumar, S. *Macro.*, **1999**, *32*, 5460.

Pressure effects on the thermodynamics of polymer blends. Kumar, S. *Macro.*, **2000**, *33*, 5285.

Effect of pressure on polymer blend miscibility: A temperature-pressure superposition. Rabeony, M.; Lohse, D.; Garner, R.; Han, S.; Graessley, W.; Migler, K. *Macro.* **1998**, *31*, 6511.

Pressure dependence of the demixing behavior in polymer blends. I. Experimental procedure. Zeuner, V.; Lentz, H.; *Macromol. Symp.* **1996**, *102*, 336.

Pressure dependence of the Flory-Huggins interaction parameter in polymer blends: A SANS study and a comparison to the Flory-Orwell-Vrij equation of state. Janssen, S.; Schwahn, D.; Mortensen, K.; Springer, T. *Macro.* **1993**, *26*, 5587.

Coil and melt compressibility of polymer blends studied by SANS and pVT experiments. Janssen, S.; Schwahn, D.; Springer, T.; Mortensen, K. *Macro.* **1995**, *28*, 2555.

Investigation of the pressure dependence of the Gibbs potential for polymer blends by means of SANS. Janssen, S.; Schwahn, D.; Springer, T.; Mortensen, K.; Hasegawa, H. *Physica B* **1995**, *213-214*, 691.

Pressure and temperature effects in homopolymer blends and diblock copolymers. Frielinghaus, H.; Schwahn, D.; Mortensen, K.; Willner, L.; Almdal, K. *J. Appl. Cryst.* **1997**, *30*, 696.

Temperature- and pressure-dependent composition fluctuations in a polybutadiene/ polystyrene polymer blend and diblock copolymer. Frielinghaus, H.; Abbas, B.; Schwahn, D.; Willner, L. *Europhys. Lett.* **1998**, *44*, 607.

Ginzburg number and phase behavior of binary polymer blends in pressure field. Schwahn, D. *Macromol. Symp.* **2000**, *149*, 43.

Pressure dependence of the miscibility of poly(vinyl methyl ether) and polystyrene: Theoretical representation. An, L.; Horst, R.; Wolf, B. *J. Chem. Phys.* **1997**, *7*, 2597.

Compressibility of two polymer blend mixtures. Hammouda, B.; Bauer, B. *Macro.* **1995**, *28*, 4505.

Pressure - Block Copolymers

High-pressure effects on the order-disorder transition in block copolymer melts. Hajduk, D.; Gruner, S.; Erramilli, S.; Register, R.; Fetters, L. *Macro.* **1996**, 1473.

Temperature and pressure dependence of the order parameter fluctuations, conformational compressibility, and the phase diagram of the PEP-PDMS diblock copolymer. Schwahn, D.; Frielinghaus, H.; Mortensen, K.; Almdal, K. *Phys. Rev. Lett.* **1996**, *77*, 3153.

Small angle neutron scattering studies on phase behavior of block copolymers. Hasegawa, H.; Sakamoto, N.; Takeno, H.; Jinnai, H.; Hashimoto, T.; Schwahn, D.; Frielinghaus, H.; Janssen, S.; Imai, M.; Mortensen, K. *J. Phys. Chem. Solids* **1999**, *60*, 1307.

Pressure Dependence of the order-to-disorder transition in polystyrene/polyisoprene and polystyrene/ poly(methylphenylsiloxane) diblock copolymers. Steinhoff, B.; Rüllmann, M.; Wenzel, M.; Junker, M.; Alig, I.; Oser, R. Stühn, B.; Meier, G.; Diat, O.; Bösecke, P.; Stanley, H. *Macro.* **1998**, *31*, 36.

Small-angle neutron scattering study of the phase behavior and mesophases of homopolymers, block copolymers and complex mixtures. Mortensen, K.; Almdal, K.; Schwahn, D.; Bates, F. *J. Appl. Cryst.* **1997**, *30*, 702.

Change of phase behavior of diblock copolymers upon application of pressure. Bartels, V.; Stamm, M.; Mortensen, K. *Polym. Bull.* **1996**, *36*, 103.

Pressure - Other Systems

Pressure-induced melting of micellar crystal. Mortensen, K.; Schwahn, D.; Janssen, S. *Phys. Rev. Lett.* **1993**, *71*, 1728.

Pressure-induced mesomorphic transition of a liquid crystalline polyester at high. temperatures. Maeda, Y.; Watanabe, J. *Macro.* **1993**, *26*, 401.

Pressure-induced melting and crystallization of poly(ethylene oxide). Li, W.; Radosz, M. *Macro.* **1993**, *26*, 1417.

Unusual pressure-induced phase behavior in crystalline poly-4-methyl-pentene-1. Rastogi, S.; Newman, M.; Keller, A., *J. Polym. Sci., Polym. Phys.* **1993**, *31*, 125.

Effects of pressure on the equilibrium properties of glass-forming polymers. DiMarzio, E.; Gibbs, J.; Fleming, P., III; Sanchez, I. *Macro.* **1976**, *9*, 763.

Pressure dependence of upper and lower critical solution temperature in polystyrene solutions. Saeki, S.; Kuwahara, N.; Kaneko, M. *Macro.* **1976**, *9*, 101.

PVT

Pressure-volume-temperature properties and transitions of amorphous polymers; polystyrene and poly(orthomethylstyrene). Quach, A.; Simha, R. *J. Appl. Phys.* **1971**, *42*, 4592.

Pressure-volume-temperature studies of amorphous and crystallizable polymers. I. Experimental. Olabisi, O.; Simha, R. *Macro.* **1975**, *8*, 206.

PVT relationships and equations of state of polymers Zoller, P. *Polymer Handbook*, 475.

Glass formation in polymers. I. The glass transitions of the poly(n-alkyl methacrylates). Rogers, S.; Mandelkern, L. *J. Chem. Phys.* **1957**, *61*, 985.

PVT properties and equations of state of polystyrene: molecular weight dependence of the characteristic parameters in equation-of-state theories. Ougizawa, T.; Dee, G.; Walsh, D. *Polymer* **1989**, *30*, 1675.

Equation of State

Statistical thermodynamics of polymer solutions. Sanchez, I.; Lacombe, R. *Macro.* **1978**, *11*, 1145.

Equation of state theories of polymer blends. Sanchez, I. *Polymer Compaibility and Incompatibility Principles and Practices*, Solc, K., Ed.; MMI Press Symposium Series Vol. 2, Harwood Academic Publishers, Chur, Switzerland, **1982**, 59.

Polymer phase separation. Sanchez, I. *Encyclopedia of Physical Science and Technology, Vol. 13*, 8th ed., Academic Press, New York, 1992.

Yeung, C.; Desai, R. C.; Shi, A.; Noolandi, J. *Phys. Rev. Lett.* **1994**, *72*, 1834.

Lower and upper critical ordering temperature in compressible diblock copolymer melts from a perturbed hard-sphere-chain equation of state. Hino, T.; Prausntiz, J. *Macro.* **1998**, *31*, 2636.

Analysis of phase separation in compressible polymer blends and block copolymers. Cho, J. *Macro.* **2000**, *33*, 2228.

Equation of state for mixtures of hard-sphere chains including copolymers. Song, Y.; Lambert, S.; Prausnitz, J. *Macro.* **1994**, *27*, 441.

Effect of monomer structure and compressibility on the properties of multicomponent polymer blends and solutions: 2. Application to polymer blends. Dudowicz, J.; Freed, M.; Freed, K. *Macro.* **1991**, *24*, 5096.

Effect of monomer structure and compressibility on the properties of multicomponent polymer blends and solutions: 3. Application to PS(D)/PVME Blends. Dudowicz, J.; Freed, K. *Macro.* **1991**, *24*, 5112.

On the large entropic contribution to the effective interaction parameter on polystyrene-poly(methyl methacrylate) diblock copolymer system. Freed, K.; Dudowicz, J. *J. Chem. Phys.* **1992**, *97*, 2105.

Lattice cluster theory of compressible diblock copolymer melts. Dudowicz, J.; Freed, K. *J. Chem. Phys.* **1994**, *100*, 4653.

Pressure dependence of polymer fluids: application of the lattice cluster theory. Dudowicz, J.; Freed, K. *Macro.* **1995**, *28*, 6625.

Influence of short chain branching on the miscibility of binary polymer blends: Application to polyolefin mixtures. Freed, K.; Dudowicz, J. *Macro.* **1996**, *29*, 625.

Energetically driven asymmetries in random copolymer miscibilities and their pressure dependence. Dudowicz, J.; Freed, K. *Macro.* **1997**, *30*, 5506.

Order-Disorder Transition

Fluctuation-induced first-order transition of an isotropic system to a periodic state. Bates, F.; Rosedale, J.; Fredrickson, G.; Glinka, C. *Phys. Rev. Lett.* **1988**, *61*, 2229.

Order and disorder in symmetric diblock copolymer melts. Rosedale, J.; Bates, F.; Almdal, K.; Mortensen, K.; Wignall, G. *Macro.* **1995**, *28*, 1429.

Complex phase behavior of polyisoprene-polystyrene diblock copolymers near the order-disorder transition. Förster, S.; Khandpur, A.; Zhao, J.; Bates, F.; Hamley, I.; Ryan, A.; Bras, W. *Macro.* **1994**, *27*, 6922.

Polyisoprene-polystyrene diblock copolymer phase diagram near the order-disorder transition. Khandpur, A.; Förster, S.; Zhao, J.; Bates, F.; Hamley, I.; Ryan, A.; Bras, W.; Almdal, D.; Mortensen, K. *Macro.* **1994**, *27*, 6922.

Density discontinuity at the microphase separation transition of a symmetric diblock copolymer. Kasten, H.; Stuhn, B. *Macro.* **1995**, *28*, 4777.

Can a single function for Chi account for block copolymer and homopolymer blend phase behavior. Maurer, W.; Bates, F.; Lodge, T.; Almdal, K.; Mortensen, K.; Fredrickson, G. *J. Chem. Phys.* **1998**, *108*, 2989.

Long-range density fluctuations in a symmetric diblock copolymer. Koga, T.; Koda, T.; Kimishima, K.; Hashimoto, T. *Phys. Rev. E, Rap. Comm.* **1999**, *60*, 60.

Block Copolymer Ordering Kinetics

Melting of styrene/isoprene block copolymers as a function of temperature and time. Hadziioannou, G.; Skoulios, A. *Macro.* **1982**, *15*, 271.

Time-resolved small-angle x-ray scattering studies on the kinetics of the order-disorder transition of block polymers. 2. Concentration and temperature dependence. Hashimoto, T.; Kowsaka, K.; Shibayama, M.; Kawai, H. *Macro.* **1986** *19*, 754.

Small-angle x-ray scattering study of ordering kinetics in a block copolymer. Harkless, C. R.; Singh, M. A.;`` À Nagler, S. E. *Phys. Rev. Lett.* **1990**, *64*, 2285.

Dynamics of structure formation at the microphase separation transition in diblock copolymers. Schuler, M.; Stühn, B. *Macro.* **1993**, *26*, 112.

Time-resolved small-anlge x-ray scattering study of ordering kinetics in diblock styrene-butadiene. Singh, M. A.; Harkless, C. R.; Nagler, S. E.; Shannon, Jr., F. R.; Ghosh, S. S. *Phys. Rev., B* **1993**, *47*, 8425.

On the microphase separation kinetics of symmetric diblock copolymers. Russell, T.; Chin, I. *Coll. & Poly. Sci.* **1994**, *272*, 1373.

Structure relaxation and metastable states at the microphase separation transition in diblock copolymers: Experiments with time-resolved small-angle x-ray scattering. Stühn, B.; Vilesov, A.; Zachmann, H. G. *Macro.* **1994**, *27*, 3560.

Nucleation and growth kinetics in diblock styrene-butadiene. Shannon, Jr., R. F.; Glavicic, M. G.; Singh, M. A. J. *Macromol. Sci – Phys.* **1994**, *B33*, 357.

Equilibrium order-to-disorder transition temperature in block copolymers. Floudas, G.; Hadjichristidis, N.; Iatrou, H.; Pakula, T.; Fischer, E. W. *Macro.* **1994**, *27*, 7735.

Metastable states below the order-disorder transition in a symmetric diblock copolymer. A time-resolved depolarized light scattering study. Floudas, G.; Fytas, G. *Macro.* **1995**, *28*, 2359.

Static and kinetic aspects of the ordering transition in thin films of diblock copolymers. Mutter, R.; Stühn, B. *Macro.* **1995**, *28*, 5022.

Nucleation and anisotropic growth of lamellar microdomains in block copolymers. Hashimoto, T.; Sakamoto, N. *Macro.* **1995**, *28*, 4779.

Finite impurity size effects on heterogeneous nucleation ocurring during in diblock copolymers. Pan, L. H.; Singh, M. A.; Salomons, G. J., Gupta, J. A. J. *Macromol. Sci. – Phys.* **1996**, *B35*, 749.

Ordering and structure formation in troblock copolymer solutions. II. Small angle x-ray scattering and calorimetric observations. Soenen, H.; Liskova, A. Reynders, K. Berghmans, H.; Winter, H. H.; Overbergh, N. *Polymer* **1997**, *38*, 5661.

Strain energy effects on the ordering process in diblock styrene-butadiene copolymer. Pan, L. H.; Singh, M. A.; Salomons, G. J., Gupta, J. A. J. *Macromol. Sci. – Phys.* **1997**, *B36*, 137.

Kinetics of superstructure formation in block copolymers. Vakulenko, S.; Vilesov, A.; Stühn, B.; Frenkel, S. *J. Chem. Phys.* **1997**, *8*, 3412.

Ordering dynamics of a symmetric polystyrene-block-polyisoprene. 1. Ordering mechanism from the disordered state. Sakamoto, N.; Hashimoto, T. *Macro.* **1998**, *31*, 3292.

Small-angle x-ray scattering study of the microphase separation transition in asymmetric diblock copolymers: A model 'B' kinetic phenomenon. Gupta, J. A.; Singh, M. A.; Salomons, G. J.; Foran, W. A.; Capel, M. A. *Macro.* **1998**, *31*, 3109.

The birefringence and mechanical properties of a 'single-crystal' from a three-block copolymer. Folkes, M.; Keller, A. *Polymer* **1971**, *12*, 222.

Optical characterization of ordering and disordering of block copolymer microstructure. Amundsen, K.; Helfand, E.; patel, S.; Quan, X.' Smith, S. *Macro.* **1992**, *25*, 1935.

Birefringence detection of the order-to-disorder trnasition in block copolymer liquids. Balsara, N; Perahia, D.; Safinya, C.; Tirrell, M.; Lodge, T. *Macro.* **1992**, *25*, 3896.

Light scattering and microscopy from block copolymers with cylindrical morphology.Newstein, M.: Garetz, B.; Dai, H.; Balsara, N. *Macro.* **1995**, *28*, 4587.

Grain growth and defect annihiliation in block copolymers. Dai, H.; Balsara, N.; Garetz, B.; Newstein, M. *Phys. Rev. Lett.* **1996**, *17*, 3677.

Evolution of microstructure in the liquid and crystal directions in a quenched block copolymer melt. Balsara, N.; Garetz, B.; Newstein, M.; Bauer, B.; Prosa, T. *Macro.* **1998**, *31*, 7668.

Calorimetry

Enthalpy of mixing of poly(2,6-dimethyl phenylene oxide) and polystyrene. Weeks, N.; Karasz, F.; MacKnight, W. *J. Appl. Phys.* **1977**, *48*, 4068.

Detection of the liquid-liquid demixing by differential scanning calorimetry. Maderek, E.; Wolf, B. *Polym. Bulletin* **1983**, *10*, 458.

Walsh, D.; Cheng, G. *Polymer* **1984**, *25*, 499.

Simultaneous differential scanning calorimetry and small-angle x-ray scattering. Russell, T. P.; Koberstein, J. T. *J. Poly. Sci., Polym. Phys.* **1985**, *23*, 1109.

Excess heat capacities for two miscible polymer blend systems. Barnum, R.; Goh, S.; Barlow, J.; Paul, D. *J. Polym. Sci., Polym. Lett.* **1985**, *23*, 395.

Studies on the heat of demixing of poly(ethylene acrylate)-poly(vinylidene flouride) blends. Ebert, M.; Garbella, R.; Wendorff, J. *Makromol. Chem., Rapid Comm.* **1986**, *7*, 65.

The relation between the microphase separation transition and the glass transition. Stühn, B. *J. Polym. Sci., Polym. Phys.* **1992**, *30*, 1013.

Direct observation of structure formation at the temperature-driven order-to-disorder transition in diblock copolymers. Stühn, B.; Mutter, R.; Albrecht, T. *Europhys. Lett.* **1992**, *18*, 427.

A high-resolution calorimetric study of the order-disorder transition in a diblock copolymer melt. Voronov, V.; Buleiko, V.; Podneks, V.; Hamley, I.; Fairclough, J.; Ryan, A.; Mai, S.; Liao, B.; Booth, C. *Macro.* **1997**, *30*, 6674.

Determination of order-order and order-disorder transition temperatures of SIS block copolymers by differential scanning calorimetry and rheology. Kim, J. K.; Lee, H. H.; Gu, Q.; Chang, T.; Jeong, Y. *Macro.* **1998**, *31*, 4045.

Excess specific heats in miscible binary blends with specific interactions. Iriarte, M.; Alberdi, M.; Shenoy, S.; Iruin, J. *Macro.* **1999**, *32*, 2661.

Scattering Studies of Polymer Blends and DiblockCopolymers

Small-angle x-ray diffraction study of thermal transition in styrene-butadiene block copolymers. Roe, R.; Fishkis, M.; Chang, J. *Macro.* **1981**, *14*, 1091.

Block copolymers near the microphase separation transition. 3. Small-angle neutron scattering study of the homogeneous melt state. Bates, F.; Hartney, M. *Macro.* **1985**, *18*, 2478

Measurement of the correlation hole in homogeneous block copolymer melts. Bates, F. *Macro.* **1985**, *18*, 525.

Neutron scattering from polymer blends under pressure. Hammouda, B.; Benmouna, M. *J. Polym. Sci., Polym. Phys.* **1995**, *33*, 2359.

High-pressure instruments for small- and wide-angle x-ray scattering. II. Time-resolved experiments. Steinhart, M.; Kriechbaum, M.; Pressl, K.; Laggner, P.; Bernstorff, S. *Rev. Sci. Inst.* **1999**, *70*, 1540.

Connell, J. G.; Richards, R. W.; Rennie, A. R. *Polymer* **1991**, *32*, 2033.

General References

Review. Russell, T. *Mat. Sci. Rep.* **1990**, *5*, 171.

Polymer Handbook, 3rd Ed. Brandrup, J.; Immergut, E., Eds. Wiley, New York, **1989**.